

Western United States Deformation: Integration of regional geologic and geodetic data into kinematic models of contemporary strain.

Mark A. Hemphill-Haley and Eugene D. Humphreys

University of Oregon, Department of Geological Sciences, Eugene, OR 97403-1272

Abstract

Penetrative dextral shear combined with gravitational collapse-driven extension provide complex deformation within the interior of the western United States and specifically within the Pacific Northwest. Geodetic observations have indicated that 9-12 mm/y of margin-parallel shear (with respect to stable North America) occurs east of the Sierra Nevada. In addition, 3-5 mm/y of west to northwest-directed extension has been observed in the central Basin and Range. The Cascadia subduction zone serves as the outlet for both sources of deformation.

We have applied finite element modeling methods to regional scale models to account for the deformation within the interior. Results show that up to 3 mm/y of dextral transpression directed toward the west-northwest occurs between the Rocky Mountain Trench and the northern Coast Ranges and includes the Lewis and Clark Lineament, the Trans-Challis Lineament, and Olympic-Wallowa Lineament. The southern Coast Ranges are moving to the west-northwest at a rate of about 7 mm/y. This results in a rotation rate for the entire Coast Range that is in agreement with estimates of Wells et al. (1998) of about 1.5°/ma of differential motion. However, the rate at which the entire mountain range is moving away from North America is about 5 mm/y less than their estimate, as a result of a pole position located in western Washington.

The Sierra Nevada is moving N50°W at 9-12 mm/y with little rotation (Hearn and Humphreys, 1998) accommodated largely by the Eastern California Shear Zone. This motion requires deformation to occur between the Sierra Nevada and the Coast Ranges. Furthermore, deformation in the Pacific Northwest is insufficient to accommodate the northern continuation of the Eastern California Shear Zone. Thus, our best estimate for the location of the remaining 3-5 mm/y of dextral shear is through the Klamath Mountains where strain is manifest as shortening and doming within the ophiolitic rocks and by westward translation of the entire block.

This southern locus of escaping deformation is particularly complex because it is located immediately north of the Mendocino Triple Junction, where the transform margin comprised of the San Andreas fault system to the south is impeding the westward collapse of the interior. The pronounced topographic relief of the Klamath Mountains may, in fact, be the deformational swale preceding the northward migration of the triple junction.

INTRODUCTION

Deformation within the Pacific Northwest of the United States consists of three poorly understood, interacting areas with different tectonic styles: 1) the Cascadia subduction zone (CSZ) where the Juan de Fuca plate (JDF) and associated fragments are being thrust obliquely beneath the Coast Ranges; 2) Basin and Range-style faults in the arc and backarc region that may be driving the forearc over the subduction zone and 3) crustal faults distributed across much of northern California, northern Nevada, Oregon and Washington that may accommodate up to 20% of Pacific-North America plate dextral shear extending northwestward from eastern California and western Nevada along the Eastern California Shear Zone (ECSZ) (Pezzopane and Weldon, 1993). These components are individually clearer elsewhere (i.e., subduction to the north, dextral shear to the south and extension to

the east) which provides strong constraint on their complex interaction in the Pacific Northwest.

It is important to realize that the deformation within the North American plate not only poses a seismic hazard in the Pacific Northwest but also affects the CSZ interface rate and style, and therefore, its hazard. Seismic hazard analysis within the Pacific Northwest has been dominated over the past decade by the potential for great earthquakes along the CSZ (Adams, 1990; Atwater, 1988; Clague and Bobrowsky, 1994; Darienzo et al., 1994; Goldfinger et al., 1994; Heaton and Hartzell, 1987; Hyndman and Wang, 1993; Kelsey et al., 1994; McCaffrey and Goldfinger, 1995; Mitchell et al., 1994; Nelson and Personius, 1991; Rogers, 1988; Savage and Lisowski, 1991; Weldon, 1991; West and McCrumb, 1988). Obvious reasons for this focus on a single seismic source include the anticipated size of the megathrust event (M_w 8 - 9+), reported short interval between events (300-600 y for entire length rupture), a relatively long elapsed time since the most recent event (~300 y), and the proximity of large Pacific Northwest population centers to the subduction zone.

Considering that Heaton and Kanamori (1984) brought the seismic potential of the PNW to the broad attention of the community little more than a decade ago, it is remarkable how much progress has been made in our understanding of the paleoseismic history and seismic hazard of this region. Continued progress on understanding PNW seismic hazard, however, is limited by the focus on the subduction zone in two important ways: 1) hazard due to crustal faults within the continent have been given relatively little attention even though their contribution to the seismic hazard of the region became evident with the 1992 Scotts Mill M_w 5.5 and 1993 Klamath Falls M_L 6.0 earthquakes. Similar faults are proposed for the Grande Rhonde Valley, Baker Valley (Simpson et al., 1993), Portland Basin (Unruh et al., 1994; Yelin and Patton, 1991) and eastern margin of the Cascades near Bend (Pezzopane and Weldon, 1993). The activities of these crustal faults are not well understood. 2) The plate tectonic setting of the subduction zone commonly is misunderstood as the JDF plate system (including Gorda and Explorer plates) subducting beneath a static North America. However, the forearc over the subducting oceanic slab actually is decoupled from North America by the crustal faults. These faults include the northern extension of the ECSZ (which accommodates Sierra Nevada block motion of about 12 mm/yr with respect to North America) and northwest-directed extension of the northern Great Basin. Together, these deformation zones act to move the forearc northwesterly with respect to North America in a manner that has been described by Wells et al. (1998) and Wang (1996). The result is that both subduction obliquity and convergence rates are affected. Current subduction models that depend on a Juan de Fuca-North America boundary condition of 40-45 mm/y of ~N60°W convergence are in error if North America deformation is not considered.

Although understanding the nature of PNW deformation is important to understanding PNW seismic risk, little information is available about strain in large portions of the Pacific Northwest due to a lack of geodetic and geologic information. A finite element model that is well constrained along its boundaries can provide insight on the distribution and style of strain accommodation.

Problems with Modeling a Simple Tectonic Margin

The magnitude of net strain across the PNW has not been appreciated by most; indeed, based solely on local geologic data there is considerable reason to doubt the existence of 10-15 mm/yr of deformation distributed across Oregon and Washington. However, the following simple and persuasive argument supports the contention that this much deformation may exist in the region. North-northwest motion of the Sierra Nevada block at 10-12 mm/yr (with respect to North America) is accommodated by deformation concentrated in ECSZ, which trends through the Walker Lane Belt east of the Sierra Nevada. This rate, verified by site velocities of well-constrained VLBI and GPS sites

located nearly on the Sierra Nevada largely has been geologically accounted for south of the latitude of San Francisco (Argus and Gordon, 1991b; Dixon et al., 1995; Hearn and Humphreys, 1998). The reportedly intact nature of the Sierra Nevada block requires deformation in the PNW to occur east of this block, whereas the nearly stationary VLBI sites at Vernal (Utah) and Penticton (British Columbia) with respect to NA require that this deformation is confined across the PNW. The exact nature and distribution of this strain is not well understood. However, considerable constraint is available by: 1) applying kinematic modeling that simultaneously includes all pertinent information and includes explicit use of known boundary velocities, faulting style and distribution, and enforces kinematic consistency and 2) comparison of modeling results with independent observations.

Modeling a Complex Tectonic Margin

Within the past decade there has been a movement to use land- and space-based geodetic data in northern California, western Washington, and southern British Columbia to resolve the CSZ strain field (Ando and Babazs, 1979; Lisowski et al., 1987; Reilinger and Adams, 1992; Rogers, 1987; Savage and Lisowski, 1991; Savage et al., 1983; Savage et al., 1991; Savage and Plafker, 1991).

Already, it has been demonstrated that vertical interseismic strain accumulation along the length of the CSZ is not uniform suggesting that the megathrust is not behaving as a heterogeneous, planar fault (Mitchell et al., 1994). Additionally, McCaffrey and Goldfinger (1995) suggest that the forearc region is deforming in a manner that prevents accumulation of sufficient interseismic strain to produce a M_w 9+ event. Madin et al. (1994) and Kelsey (1990) describe onland deformation of late Pleistocene marine terrace deposits. Although it is tempting and proper as a first effort, to model these observations simply by segmenting the subduction zone (Verdonck, 1995), enough is now known to allow consideration of the complexities described here. To be more specific about western U.S. deformation that bears on the PNW: earlier estimates of convergence between Juan de Fuca and North America have not considered that "stable" North America is not located along the western North America margin. In fact, a large portion of the western interior of North America is actively deforming, as evidenced by: 1) fault slip data and seismic moment tensors suggest that southcentral and southeastern Oregon are moving to the northwest at about 6 mm/y (Pezzopane, 1993; Pezzopane and Weldon, 1993). This estimate accounts for only 40% to 50% of the dextral shear associated with the northern part of the ECSZ; 2) VLBI estimates at Ely, NV (Dixon et al., 1993; Dixon et al., 1995) and slip-rate and GPS data along the Wasatch fault (Martinez et al., 1998; Smith and Braile, 1993) indicate that the eastern part of Basin and Range province is extending to the WSW at about 4 to 5 mm/y, away from eastern portions of North America. This direction is almost perpendicular to Pacific-North America transform motion and 3) two locally significant earthquakes that have occurred in western Oregon in this decade, the 1993 (M_w 5.6) Scotts Mill event and the 1993 (M_L 6.0) Klamath Falls event.

Complicating matters further, estimates of Pacific-North American relative plate velocity has been modified in recent years. As a result of path integration of multiple fault slip-rates across the southwestern U.S., Humphreys and Weldon (1994) estimate a Pacific-North America plate rate (4.8 ± 0.2 cm/y) that is in agreement with RM2 and NUVEL-1 but is directed $\sim 7^\circ$ counterclockwise to these models. DeMets et al. (1994) suggest new rates that are approximately 5% slower than previous estimates. Both of these changes would decrease convergence rates for Juan de Fuca-North America.

Hence, if we want to understand JDF subduction velocity at a higher level of accuracy, we need to take the next step and incorporate the complexities.

Purpose

The objective of this research is to characterize Pacific Northwest deformation resulting both from the accumulation of interseismic strain along the CSZ and from other sources of strain not directly attributable to subduction zone interaction. It consists of integrating geologic, geodetic and geodynamic data to provide a kinematic description of the contemporary strain in the region.

We attempt to resolve several outstanding issues regarding Pacific Northwest tectonics and seismic hazards. They include: 1) a kinematic assessment of the distribution of strain that accommodates the northern extension of the ECSZ within northern California, Nevada, Oregon and Washington; 2) an estimate of the relative convergence velocities between oceanic plates and North America across the CSZ, as represented by the velocity of the Coast Ranges block with respect to the oceanic plate. We compare scenarios where western North America is attached rigidly to the stable interior of North America (plate-rate model) and where western North America deforms above the subduction zone (our preferred model); 3) development of a kinematic map depicting deformation within the interior of the western U.S. which may influence deformation along the subduction zone and 4) construction of a map that depicts strain within the western U.S., specifically within areas where little contemporary deformation information is currently available.

Approach

The project consists of integrating geologic and geodetic data to provide kinematic (and locally dynamic) descriptions of contemporary strain, including both the (variably straining) CSZ and the backarc region. We use a 2-D finite element code to construct kinematically-consistent map-view models of the Pacific Northwest. Because the quantity and quality of data are always improving, our model is designed to easily incorporate changes in the data set.

All modeling is motivated by a desire to include information that usually is ignored, and to handle information correctly (i.e., satisfying the relevant equations). The often-ignored constraint that we include in kinematic modeling is that of the "compatibility condition". In particular it is geometrically required that the integrated strain along any path connecting two points (and therefore on any surface, such as the Earth's) yields the relative velocity of the end-point with respect to the start-point (as discussed by (Minster and Jordan, 1987)). It is not possible, for instance, to have thrust faulting at depth without having an identical accounting of this deformation at the Earth's surface. Nor is it possible to have the ECSZ accommodate 10 mm/yr while eastern Oregon accommodates only 5 mm/yr, without having some physical means for accommodating this difference. Dynamic modeling adds the requirement that forces balance; if forces do not balance, the model is unphysical. This dynamic constraint is as meaningful as requiring that cross sections balance. However there is a practical problem with this requirement: observations involve displacements, which are related to stresses through material properties that are not perfectly known. In spite of this, elastic constants are known well enough to restrict the class of admissible model solutions, and orientation information (stress and strain) generally is quite robust even when absolute values of stress are not certain.

KINEMATIC AND DYNAMIC SETTING OF THE WESTERN UNITED STATES

The modern plate margin of western North America is dominated by the approximately 5400 km-long Pacific-North American transform plate boundary that extends from the Gulf of Alaska to south of the Baja Peninsula (Figure 1). The margin is comprised of two large transform faults, the Queen Charlotte Fault (approximately 1200 km long) to the north and the San Andreas Fault system (including the spreading Gulf of California) to the south (approximately 2800 km long). Dextral shear along the transform

faults juxtaposes the oceanic Pacific plate against the continental North American plate. A releasing right-step between the two faults coincides with the CSZ where the waning remnants of the Juan de Fuca plate and lesser Gorda and Explorer plates are thrust obliquely beneath North America. In comparison to the overall length of the transform margin, the subduction zone is actually relatively small (Figure 1). Although the plate boundary is relatively simple, the western margin of North America tectonically is very complex. Not only is there broadly distributed strain associated with the transform and subduction zone, but the interior of the continent is gravitationally collapsing.

The tectonic configuration of northern transform margin along the Queen Charlotte Fault has remained relatively stable for at least the past 30 Ma (Atwater, 1989). Conversely, the southern transform margin has undergone substantial modification in the past 30 Ma, essentially transforming from a subduction- to strike-slip-bounded margin through a series of Farallon- to Pacific-micro-plate transfers (Atwater, 1970; Atwater, 1989; Atwater and Stock, 1997; Severinghaus and Atwater, 1990). The contemporary southern transform margin extends from Mendocino to Rivera and continues to migrate northward, led by the Mendocino Triple Junction.

Fundamentally, the warm continental lithosphere of western North America is inherently weak relative to the strong oceanic lithosphere of the Pacific plate. This has resulted in large amounts of diverse deformation such as Eocene contraction (for example Laramide deformation within the entire North American Cordillera (Dumitru et al., 1991; Hamilton, 1988; Humphreys, 1995; Livaccari, 1991)), late Cenozoic extension (for example the contemporary Basin and Range province), establishment of inland shear zones associated with the plate margin tectonics (for example, ECSZ). This latter issue can be best illustrated by the fact that although the Pacific plate is moving in a direction of about N45° to 38°W at a rate of almost 4.8 cm/yr relative to North America only about two-thirds of that motion can be attributed to the San Andreas fault (Humphreys and Weldon, 1994; Minster and Jordan, 1987; Pezzopane and Weldon, 1993). The rest of the shear deformation has been transferred east of the Sierra Nevada (Humphreys and Weldon, 1994; Pezzopane and Weldon, 1993).

Interior deformation is dominated by the post-Laramide collapse of the high-standing, thickened lithosphere (Hamilton, 1988; Humphreys, 1995; Jones et al., 1996). The Laramide Orogeny occurred during the late Cretaceous to early Paleocene when young, buoyant oceanic lithosphere of the Farallon plate was subducted beneath North America. The introduction of a more buoyant slab resulted in a shallower subduction angle. Contraction occurred far inboard of the subduction zone with the majority of deformation located in the northern and central Rocky Mountains (Hamilton, 1988). Horizontal compressional stresses were sufficient to cause thickening of the lithosphere and resulted in a region of high potential energy. Once a steeper subduction angle was re-established along a new plate margin to the west, and traction between the sub-horizontal slab and the North American lithosphere diminished, the high-standing interior began to collapse. The path of least resistance was toward the poorly-coupled subduction margin free-face (Figure 2).

The contemporary deformation within the continental lithosphere of western North America is actually the result of an interplay between the stresses and strengths associated with the expanding transform and diminishing subduction margins and the ongoing "gravitational collapse" of the interior. For simplicity, we consider two orientations of deformation within the continent, one that parallels the margin and one that is directed normal to the margin. We also consider the two types of margins that are present, the relatively long transform and the smaller subduction zone. Along the transform, margin-parallel deformation is dominated by dextral shear driven by Pacific/North American plate motion. Margin-normal motion, driven by westward collapse of the high standing continental interior, is impeded along the transform by its nearly vertical interface and the unyielding massive, strong Pacific plate (Figure 3). Along the subduction zone within the United States, margin-parallel deformation occurs as a result of the oblique convergence of the Juan de Fuca plate relative to North America and due to the dextral shear imposed

across the step-over by the transform margin. Within Canada, where the convergence direction is nearly normal to the margin, the margin-parallel motion is due solely to the regional transform interactions. Margin-normal motion of western North America is greater near the subduction zone than along the transform because the subduction fault is at a low-angle and is weakly coupled (Wang et al., 1995). This is where North America deformation, which is pervasive in the interior of the western U.S., is accommodated. Thus, the subduction zone allows the North American plate to move westward over the Pacific plate, both as a result of the subduction of the sinking oceanic slab and the westward collapse of North America. A further consideration is that deformation in the region around the subduction zone is influenced by the presence of the right-step in the transform margin. The dextral plate motion and geometry of the right-step add a component of dilation in the region of the subduction zone in spite of the shortening that is occurring at the subduction zone.

FINITE ELEMENT MODELING OF KINEMATIC DEFORMATION

Using the finite element program Patran (MSC, ver.7.6), we model the western U.S. as a two-dimensional plate separated into blocks by weak zones representing faults and fault zones. This model is deformed with prescribed block velocities, which are applied by assigning the displacements that accumulate during a 1 year period and boundary conditions derived from global plate models. We prescribe velocities for selected blocks that represent physiographically distinct entities such as the Pacific plate, Sierra Nevada block, and Juan de Fuca plate based on data derived from geologic and geodetic observations. The finite element modeling solves for the deformation field that minimizes net elastic strain energy of the entire model, where local strain energy density is given by the tensor dot product of stress and strain.

To understand this modeling approach better, recall that stress is linearly related to strain through a material's elastic modulus. One then recognizes element strain energy density to be a measure of squared misfit, and the model of minimum total strain energy can be viewed as a least squares solution to the question: what velocity field best satisfies the applied constraints. In this view, the elastic moduli of an element are the parameters that determine the relative weight given to that element in the global minimization of strain energy (Hearn and Humphreys, 1998; Saucier and Humphreys, 1993). It is important to recognize that with this kinematic modeling, stress and strain do not represent actual lithospheric values; rather, they quantify the degree of block misfit that occurs in 1 year under the prescribed boundary and block velocities. If one were interested in actual lithospheric stress, an initial (large) stress field and contributions resulting from basal tractions and finite fault strength would need to be included.

As an example of kinematic modeling, consider a map cut into pieces (cuts representing faults) that can be deformed with a set of displacements so that no overlap or gaps form. Our finite element simulation of this case would result in no block deformation, and stress and strain would be zero everywhere. If the prescribed fault slip requires the creation of overlap and gaps, then one can find a "best" solution by minimizing the net area of overlap and gap. The general idea behind the finite element modeling is that where block motion cannot occur with the prescribed faults and velocities, elements strain to accommodate inconsistencies. The strain energy is used as a measure of kinematic inconsistency, much like overlap and gap area can be used to measure kinematic inconsistency in the cut map example.

The finite element approach to kinematic modeling allows for a simultaneous inclusion of information about faults (fault location, geometry, faulting style, and slip rate), geodetic data (i.e., relative point velocities), and far-field velocities (e.g., relative plate velocity). By incorporating these data types simultaneously, this modeling technique provides significant constraint. The description of the model region as blocks separated by fault zones has proven especially useful in incorporating geologic information into models

of regional deformation because, where deformation is block-like, important kinematic constraint is provided by fault location, orientation and slip velocity. This fault-and-block modeling is justified by observations that deformation in most places is dominated by slip on major faults: far-field velocities are attained by summing the geologically inferred slip rates on major faults (Humphreys and Weldon, 1994). Plate and large block rotations are calculated using large-scale plate motions (Argus and Gordon, 1991b; DeMets et al., 1990; DeMets et al., 1994; DeMets et al., 1987; Gripp and Gordon, 1990; Riddihough, 1984). However, there are regions where deformation is known to be distributed on folds and faults spaced too closely to be represented well by our model. For instance, ECSZ is one place where distributed deformation appears to occur at significant rates. Where we recognize or suspect kinematically important rates of distributed deformation to be occurring, we simply include a zone of low-strength elements. This allows deformation to occur within those elements while contributing little strain energy to the strain energy sum, thereby effectively eliminating the kinematic influence of the local structures in these areas.

Model Scale

The finite element model boundaries were constructed so as to encompass all of the geologic entities that we considered important to the tectonic setting of the Pacific Northwest. Because we consider the transform margin and deformation of the interior to be important tectonic components we have extended the model boundaries well beyond the region that might typically be considered within the vicinity of the Pacific Northwest (Figure 4). The model extends from the Rivera plate to the south to the northern Queen Charlotte Fault to the north. The western margin of the model extends beyond the Juan de Fuca Ridge and includes the Pacific plate. The eastern margin of the model extends east of the Rocky Mountains and Colorado Plateau to include a portion of the "stable" North American plate.

We constructed the Pacific Northwest portion of the model with sufficient detail to be able to observe individual zones of faults and geologic provinces. Limitations on geologic data prohibited the development of an individual fault-scale model for the region.

Model Geometry and Mesh

The finite element code that we have used for this analysis allows for development of geometric shapes that can be used to define specific regions of interest. The finite element mesh, loads and material properties can then be associated with individual geometric entities. We selected geometric shapes (Figure 4) to depict tectonic domains (e.g. oceanic plates, the Coast Range), deformation zones and fault zones (e.g. the Cascadia Subduction Zone, San Andreas Fault Zone, Rio Grande Rift) and stable areas (e.g., Colorado Plateau, Sierra Nevada, "stable" North America). We constructed the model geometries using a base map depicting geographic boundaries and late Cenozoic faults (Figure 4).

The model was meshed using Triangular elements (Tria3). We increased element density in areas of geometric and geologic complexity, along significant tectonic boundaries, and in areas where locally-significant strains were anticipated (Figure 5).

Material Properties

We have assigned five different elastic constitutive properties to crustal block geometric entities, and their associated elements, that reflect their relative deformational characteristics. We have assigned strengths with the use of Young's modulus E and we vary compressibility with the use of Poisson's ratio ν (Figure 6). Values for E vary over a wide range of values, the weakest crustal domains are assigned values of 0.1 while the strongest (i.e., oceanic plates, stable North America) have values of 10,000. Deformation zones within

the continental plate have values of E that vary from 1 to 10. The crustal blocks all have a ν of 0.25 which is typical for crustal rocks. Faults have been assigned slightly different elastic properties to reflect their deformational differences from the crustal rocks. For instance, oceanic transform faults are assigned values of $E = 0.01$ to provide weakness and ν of 0.49 to reflect the non-dilatational form of that style of fault. Conversely, oceanic ridges are weak ($E = 0.01$) and compressible ($\nu = 0.01$). Finally, reverse faults, such as the Cascadia subduction zone have been modeled to have slightly more strength ($E = 0.05$) than transform and normal faults but are compressible ($\nu = 0.01$). These variations in material property allow deformation to concentrate with the actual deformation zones and choice of value is guided by comparing model prediction with observation where possible. Regardless of choice of Young's Modulus and Poisson's Ratio, the compatibility constant (discussed above) will always be satisfied.

Applied Velocities -

To provide a kinematic description of the deformation field of the western U.S., velocities (in units of mm/y) were applied to selected blocks (Table 1, Figure 7). Some velocities, such as those for the Pacific and Juan de Fuca plates, were assigned based on global plate estimates (Argus and Gordon, 1991b; DeMets et al., 1990; DeMets et al., 1994; DeMets et al., 1987; Dixon et al., 1995; Gripp and Gordon, 1990; Minster and Jordan, 1987; Riddihough, 1984). Local velocities were based on short-term observations at VLBI and GPS sites (Bennett et al., 1998; Martinez et al., 1998; Shen-Tu et al., 1998); strain-estimates (Kreemer et al., 1998; Savage, 1983; Savage and Burford, 1970; Savage et al., 1983; Savage et al., 1991; Savage et al., 1995); geological observations (Hemphill-Haley et al., 1998a; Hemphill-Haley et al., 1998b; Hemphill-Haley et al., 1996; Pezzopane and Weldon, 1993); paleomagnetic results (Magill et al., 1982; Wells et al., 1998), and results based on a combination of finite element modeling and geodetic data (Hearn and Humphreys, 1998; Wang, 1996).

We constructed the model using the least number of input velocities that still constrained deformation. Paired velocities were assigned to blocks so that rotations could be applied (Figure 7). The paired velocities were calculated based on Euler pole rotations and in such a manner that rigid blocks were not strained. Velocities applied to the model are listed in Table 1. Specific blocks where velocities were applied are discussed below.

MODELING THE WESTERN U.S.

We incorporate three iterative steps to develop the kinematic model of the western U.S., input, modeling, and evaluation. We initialize the model by prescribing velocities to select blocks based on geodetic observations, global plate estimates and geologic rates. We then assign material properties to individual blocks and zones to best depict the deformation styles and rates that we anticipate from observations. The model is then run, producing the deformation field of minimum strain energy (as described above) while utilizing the prescribed inputs. We then evaluate the model results and compare them with observations of tectonic style and geologic/geodetic velocities. Based on this comparison, the input velocities or material properties are adjusted and the model is run again.

Using this iterative process we have produced models that represent several possible tectonic scenarios. They include:

1) Our Preferred Model: This model is the result of numerous iterations which consider variations in plate and block motions and material properties. The preferred model is most consistent with observations of deformation rate and style throughout the western U.S. The primary inputs into the model include: a Pacific plate velocity that corresponds to Nuvel-1a, the Oregon-Washington Coast Range block rotates about Euler pole (λ 46.1°N, ϕ 121.0°W,

ω $-1.51^\circ/\text{m.y.}$), the Sierra Nevada block rotates about the Euler pole defined by Hearn and Humphreys (1998) (λ 13.4 , ϕ 154.4°W , ω $-0.16^\circ/\text{m.y.}$), motion of interior blocks in the northern Basin and Range, Snake River Plain and Colorado Plateau reflects the influence of gravitational collapse.

2) Passive Interior Model: velocities are similar to the preferred model except interior blocks do not have prescribed velocities but instead move in accordance with margin related motions.

3) Adjusted Pacific Plate Azimuth Model: A velocity reported for the Pacific plate by Humphreys and Weldon (1994) is applied instead of the Nuvel-1a velocity. This results in an azimuth for the Pacific plate near the southern California coast that is approximately 7° counterclockwise to that for Nuvel-1a. All other velocities are consistent with the preferred model.

Plate Velocities

Velocities are applied to several “rigid” plates ($E = 10,000$) to constrain the velocities of the model boundaries. These velocities are based primarily on estimates derived for global plate rates (Argus and Gordon, 1991b; DeMets et al., 1990; DeMets et al., 1994) and geodetic and geologic observations. All velocities applied in this model are with respect to a “stable” North America reference.

Stable North America - the eastern margin of the model is constrained by a rigid North America plate that is not moving with respect to the right boundary of the model. This is based on GPS and VLBI observations showing that stations located east of the Rocky Mountains and Rio Grande Rift are moving negligibly with respect to the east coast of North America (Argus and Gordon, 1996).

Pacific Plate - the rigid Pacific plate forms the western portion of the model. We have based velocities for our model on Nuvel-1a estimates for Pacific plate motion (DeMets et al., 1990; DeMets et al., 1994). The plate moves counter-clockwise with a rotation rate (ω) of $\sim 0.75^\circ/\text{m.y.}$ about an Euler pole located at $\lambda = 48.7^\circ$, $\phi = 78.2^\circ$ (Table 1). An alternative Pacific plate velocity has been proposed by Humphreys and Weldon (1994) based on path integration of geologically-derived fault slip rates within the western U.S. This estimate provides a similar rate to Nuvel-1a but differs in that the Pacific plate azimuth is about 7° counterclockwise to the Nuvel-1a estimate.

Juan de Fuca, Gorda and Explorer Plates - We have applied velocities to two of the oceanic plates along the western margin of the Cascadia subduction zone in order to estimate convergence rates along the subduction margin. We model the Juan de Fuca and Explorer plates as rigid oceanic plates and the Gorda plate as deforming lithosphere.

The Juan de Fuca rate is based on estimates by Riddihough (1984) using analyses of magnetic anomalies and transform faults. We calculate a Juan de Fuca Euler vector of $\lambda = 29.4^\circ$, $\phi = 117^\circ$, $\omega = -1.09$ (i.e., clockwise) (Table 1).

Based on velocity field estimates derived from earthquake strain rates, Kreemer et al. (1998) suggest that the Explorer plate actually serves as a “pseudo-plate” boundary zone between the Pacific and North America plates. They conclude that approximately $50 \pm 30\%$ of the Pacific-North America plate rate occurs within the Explorer plate. Our rate estimate includes a rotation rate (ω) of $0.75^\circ/\text{m.y.}$ (Table 1).

The young, warm and weak Gorda plate is being deformed internally as expressed by the incompatible geometries of the Mendocino and Blanco transform faults (Denlinger, 1992; Stoddard, 1987; Stoddard, 1991; Wilson, 1989). We model the Gorda plate as a

relatively weak zone and do not apply a velocity to it; instead, we allow the better constrained plates around it control its deformation.

Continental Blocks Along the Plate Margin

Although this is a kinematic model we can address some of the dynamic processes acting on the western U.S.. For instance, simple transform entrainment is a passive process that acts on a variable strength margin. If gravitational collapse were not important, then there would be no need to prescribe the velocities of blocks within North America, yet we must do just that.. The applied velocities can be viewed as a proxy for the gravitational driving force needed for collapse. We can then compare these two models to assess the role of shear penetration and gravitational collapse.

When modeling to investigate effects of gravitational collapse, we have minimized the boundary constraints applied to the interior of the model. When modeling the purely passive case, velocities for all interior blocks (except for those directly along the margin) are left free.

We have prescribed velocities to four important crustal blocks that lie along the Pacific-North America plate margin, they are British Columbia, the Coast Ranges of Oregon and Washington, the Sierra Nevada and Colorado Plateau. These velocities are well-constrained and provide kinematic control for the deformation of North America.

British Columbia - This portion of the plate margin is undergoing considerably less deformation than the margin and interior to the south. The Canadian Rocky Mountains, although high-standing, are not collapsing toward the Pacific plate. The reason for this is unknown but it is possibly due to several factors: 1) British Columbia is bounded to the west by the Queen Charlotte transform which, like the San Andreas, serves as a barrier to westward expansion, 2) the "flow" of western U.S. lithosphere, due to dextral-shear forces and gravitational collapse, is northward toward the CSZ, thus creating a pressure against southern British Columbia that impedes its collapse toward the south, and 3) the mantle beneath much of British Columbia is stronger than in the western U.S. interior as inferred by high seismic velocities (van der Lee and Nolet, 1997) and low heat flow (Figure - 8).

We have applied velocities to the British Columbia block (Table 1) to provide a small clockwise rotation to the block ($\omega = 0.02^\circ/\text{m.y.}$). This rotation is consistent with dextral shear at the western margin, thrust faulting in the northern British Columbia Rocky Mountains and diminished velocities toward the stable interior.

Coast Ranges - The Coast Range block lies between the accretionary prism of the CSZ to the west and the Cascades volcanic arc of Washington and Oregon to the east (Figure 6). Based on paleomagnetic, geologic and finite-element modeling data (McCroory, 1996; Wang, 1996; Wells et al., 1998), the Cascadia fore-arc has rotated clockwise at a rate of about $1.5^\circ/\text{m.y.}$ for at least the last 12 m.y. (Magill et al., 1982). In addition, the velocity for the Coast Ranges also includes a component of northward motion based on geologic evidence (Magill et al., 1982) and finite-element modeling of subzone dynamics (Wang, 1996). Based on geologic arguments, the initial input velocity for our model was based on an initial Euler vector estimated by Wells et al. (1998) at $\lambda 48.5^\circ\text{N}$, $\phi 118.7^\circ\text{W}$, $\omega -0.91^\circ/\text{m.y.}$ Wells (1998) provided a revised vector ($\lambda 46.867^\circ\text{N}$, $\phi 119.962^\circ\text{W}$, $\omega -1.168^\circ/\text{m.y.}$) that we also tested, however, kinematic inconsistencies resulting from both vectors forced us to revise the vector to $\lambda 46.1^\circ\text{N}$, $\phi 121.0^\circ\text{W}$, $\omega -1.51^\circ/\text{m.y.}$ (Table 1).

Choice of the Coast Range block velocity has a significant influence on the western U.S. deformation.. Nearly all of the dilation that occurs in the western U.S. is accommodated by the westward motion of the Coast Range block. Although the mechanism responsible for the block's motion is poorly understood (e.g., is it being pushed from the east or pulled from the west), the rate of expansion of the interior is dictated largely

by the rate at which the Coast Range block moves. The block's motion also directly impacts the convergence rate along the CSZ, between the JDF system and North America plate. Most estimates of convergence have included only the JDF plate rate, assuming that the upper plate is fixed. However, the westward migration of the Coast Range toward the subduction zone will affect the rate.

Sierra Nevada - The Sierra Nevada block lies between the SAF and ECSZ (Figure 6). Motion of the Sierra Nevada can be attributed to a combination of plate margin shear traction and gravitational collapse (Hearn and Humphreys, 1998). The velocity estimate used in this model is derived from finite element modeling and kinematic constraints on faulting of the southern Sierra Nevada and Walker Lane Belt (Hearn and Humphreys, 1998). Two velocities applied to the Sierra Nevada (Table 1) provide a small counterclockwise rotation ($0.16^\circ/\text{M.y.}$) to the block. Other models for Sierra Nevada motion include a larger amount of rotation for this block (Argus and Gordon, 1991a).

The velocity estimated by Hearn and Humphreys (1998) is based on the assumption that the VLBI/GPS site at Quincy is located on the Sierra Nevada block and that the Sierra Nevada block is rigid. However, numerous north-northwest-trending strike-slip and normal faults lie within the northern Sierra Nevada block and in the transition to the Modoc Plateau, perhaps indicating that the northernmost portion of the block is not rigid. The implications of such a scenario depend on the nature of any such deformation but any reasonable faulting activity would increase the rotation rate of the Sierra Nevada block.

Colorado Plateau - The essentially non-deforming Colorado Plateau is rotating counterclockwise at a slow rate. This is possibly due to lowered horizontal compressive stresses to the west as a result of extension. Hamilton (1988) suggests that about $3-4^\circ$ of post-Laramide rotation of the Colorado Plateau provides the east-west extension of the Rio Grande Rift and the north-south contraction found in the Uinta Mountains to the north. Accordingly, we apply an Euler vector of $\lambda 41.65^\circ\text{N}$ $\phi 104.75^\circ$ $\omega \sim 0.1^\circ/\text{m.y.}$ to the Colorado Plateau block.

Additional Interior Blocks

Eastern Snake River Plain - The Yellowstone hotspot lies just northeast of the Snake River Plain (SRP). Yellowstone has the highest potential energy of any location within North America (Figure 2). The eastern SRP is essentially devoid of faults suggesting that it is behaving as a single block. The cumulative slip rate of faults across southern Idaho is comparable to that of the Wasatch front. Thus we assume that the SRP is moving westward, away from the highstanding Yellowstone plateau, at a rate of ~ 3 mm/y, similar to that observed near the Wasatch Front (Martinez et al., 1998). We have prescribed a small clockwise rotation ($w = 0.44^\circ/\text{m.y.}$) to the block to allow the western end to move toward the northwest to satisfy kinematic constraints of surrounding faults (Table 1, Figure 7).

Idaho Batholith and John Day Region - In order to provide consistent strain observations, two blocks within the Pacific Northwest were prescribed velocities. The Idaho Batholith moves westward with a clockwise rotation rate of $0.2^\circ/\text{m.y.}$ about a pole located at $\lambda 48.6^\circ\text{N}$, $\phi 113.5^\circ\text{W}$ (Table 1). This allows faults north of the SRP and east of the Idaho Batholith to slip. Also, the John Day region, appears to be moving toward the northwest at a rate of 1-3 mm/y. Recent paleoseismic trenching along a portion of the Yakima fold belt (West et al., 1996) to the north of the John Day region suggests that a single thrust fault in that zone (Saddle Mountain anticline) may have up to 0.5 mm/y horizontal shortening. There are four other similar structures in the zone and shortening related to folding has not been calculated. Thus, estimates in the range of 1-3 mm/y of N-S shortening for the area are consistent with the fold belt rates.

There is still a large-fraction of the western U.S. where little or no strain information exists. For those areas we rely on the model boundary constraints and the concept of the compatibility constant to provide self-consistent interpolated strain estimates

MODEL RESULTS

Model results consist of nodal velocity and element centroid strain. The results correspond to the deformation field of minimum energy, under the constraint that prescribed velocities are satisfied, as discussed above. The results can be thought of as an instantaneous snapshot of the velocity and strain fields for the western U.S. To illustrate the deformation, we show model velocity and isotropic strain Δ . Because modeling is 2-D (plain strain), Δ represents change in area:

$$\Delta = (a_f - a_0)/a_0$$

where a_0 is the original area and a_f is the final area. For our models, the percentage of strain is reported (where positive values are dilation, that is, a gain in area due to extension).

The discussion below begins with a description of the results of the model which we feel most satisfactorily describes the deformation field of the western U.S. We then describe why the model is preferred over two models with significantly different initial conditions.

1) Preferred model - Our preferred model satisfies most geologic and geodetic observations for western U.S. deformation rates (Figure 9) and styles (Figure 10). The largest velocities are confined to the oceanic plates and the plate margin of North America. An enlargement of the western part of the model area shows the details of the margin velocities (Figure 11). At the latitude of about 35°N, almost all of the Pacific-North America plate motion is taken up within a zone that is less than 300 km wide. There is an abrupt, large decrease in velocity from west to east from about 40 mm/y to 5 mm/y immediately across the ECSZ in southern California.

Conversely, at the latitude of about 40°N about 75% of the plate motion is accommodated within the San Andreas fault system over a zone less than 100 km wide. Most of the remaining ~25% of motion is taken up by the northward motion of the Sierra Nevada block. A sharp velocity gradient (from about 12 mm/y to 7 mm/y) occurs across the ECSZ within a narrow zone less than 150 km wide in northern California and western Nevada. Farther inland, within the Basin and Range province, the velocity slowly decreases from about 7 mm/y near western Nevada to less than 1 mm/y along the eastern margin of the province at the northern Colorado Plateau, over a distance of about 700 km.

North of the Mendocino Triple Junction (MTJ) and the southern end of the CSZ, the northern end of the Sierra Nevada block is no longer constrained by the Pacific plate transform margin. Thus, much of the northwest-directed deformation east of the ECSZ moves to the west, through the Klamath Mountain province and out over the CSZ (Figure 11). The deformation zone is about 300 km wide extending from north of Cape Mendocino to the northern Siskiyou Mountains. The velocity gradually decreases along a line normal to the trend of the zone from 12 mm/y at the Northern Sierra Nevada to less than 4 mm/y at about Salem. A portion of the deformation within this zone is accommodated by the clockwise rotation of the Coast Range block. The southern end of the block moves toward the west-northwest at about 7 mm/y (Table 1).

North of latitude 45°N velocities diminish to less than 3 mm/y and become more north-directed, in part due to the north-directed translation of the Coast Range block in addition to its rotation (Table 1). This translation may be the result of the northward component of oblique convergence along the poorly coupled CSZ (Wang, 1996) and also due to the northwest-directed deformation from within the North American plate. Much of the deformation appears to converge on the Olympic Peninsula of Washington. This is

partly due to the buttress effect caused by the lower velocity British Columbia block to the north and the weak accretionary flysch material that comprises the Olympic Peninsula (Brandon et al., 1998).

The isotropic strain map from this model (Figure 10) provides additional insight about the style of deformation that is occurring. The margin related deformation is the location of large amounts of shear with local differences mainly caused by geometrical-irregularities and complications due to North America plate deformation. The transform margin has a large dextral releasing bend in the area of the Gulf of California (South of latitude 35°N). At the Big Bend of the SAF the left-stepping fault undergoes transpression with large amounts of contractional strain (exceeding 12%/m.y.) occurring in the vicinity of the Transverse Ranges. The northern San Andreas is also largely transpressional but with smaller contractional strains. Inversion of strain within the East Bay Hills suggests that those structures are transpressional (Unruh and Lettis, 1998), however, this may be a localized strain that is superimposed on the larger transtensional field (William Lettis, personal communication, 1998). The northernmost SAF is also transpressional with a small amount of transtension located near Point Delgado possibly where the fault turns more northerly before ultimately merging into the Mendocino fault.

The map shows the large contractional strains (>200%) associated with JDF plate system subduction. Two prominent areas of contractional strain are also evident at the southern and northern ends of the CSZ where they protrude into the North American plate. The southern zone coincides with the Klamath Mountains province where deformation associated with the northern extent of the ECSZ may be directed. To the north, the large zone of contraction is centered on the Olympic Mountains with its northern margin across Vancouver Island. An arm of the eastern part of the contractional zone extends southward along the Northern Cascades arc and terminates in southern Washington near the terminus of observed contraction in the arc (Wells et al., 1998).

Moving inland, the prominent zones of extension that diverge northward into fingers from the ECSZ correspond to zones of relatively high rates of extension in the Basin and Range, along the eastern front of the Yellowstone Plateau, the Wasatch Front and the Rio Grande Rift (Figure 10). The pattern of deformation is similar to that postulated by Pezzopane and Weldon (1993). Within the northernmost Basin and Range of Oregon several zones of moderate extension (ranging from ~1% to 5%/m.y.) occur. Within the Central Oregon zone of faulting described by Pezzopane and Weldon (1993) a northwest-trending zone of extension coincides with an area of Holocene volcanism and faulting (Hemphill-Haley et al., 1996). Farther to the east, the northeast-trending Steens fault zone shows the diminishing extension of the northeastern part of the northern Basin and Range.

A noticeable zone of contraction (up to 3%/m.y.) occurs along the Olympic-Wallawa Lineament (OWL) of southern Washington and northeastern Oregon (Hooper and Conrey, 1989; Mann, 1991). This zone is located at the Yakima fold belt and is the result of collision by the stronger John Day region to the south as it moves northwest toward the subduction.

The Rio Grande Rift is the result of movement of the Colorado Plateau toward the west. The northern margin of the plateau is pinned against the stable interior of North America while the southwest boundary is unconfined as a result of the west-northwest motion of the Basin and Range. This results in a small clockwise rotation of the Colorado Plateau and small strains within the Rio Grande Rift (associated velocities across the Rift are less than 1 mm/y (Figure 9)).

Our preferred model deforms the continental interior in a manner that is consistent with observations in contrast to the "passive interior" model. The passive model tests whether plate margin forces are sufficiently large to deform the continental interior. It results in interior velocities (Figure 12) and deformational styles (Figure 13) that are considerably different from observations. In particular, areas north of the Snake River Plain, near Yellowstone, within the Yakima fold belt and along the Rio Grande Rift have negligible strain.

Our preferred model provides deformation rates and styles along the margin that are more consistent with observations than the "Adjusted Pacific Plate Azimuth" model. The more west-directed model results in transtension along most of the SAF (Figure 14) with the exception of the Big Bend region which has a smaller area of contraction.

DISCUSSION

In addition to providing deformation maps of the continental interior, careful modeling of the interior deformation was important to constrain Pacific Northwest kinematics. We now turn our attention to the primary goals of this study which are to provide a kinematic assessment of the distribution of strain that accommodates the northern extension of the ECSZ and to compare the relative convergence velocities between subducting oceanic plates and North America across the CSZ using information about the deforming upper plate which is absent in plate-rate models.

As discussed above, there has been little contemporary geodetic or seismologic information that lends insight about the continuation of shear strain northward from the ECSZ. Likewise, identification of strain distribution using seismic moment is limited because seismicity production in the Pacific Northwest (especially in Oregon and northern Nevada) is extremely low (Pezzopane and Weldon, 1993).

Our preferred model indicates that perhaps as much as 5 mm/y of deformation is being shunted through the Klamath Mountains along the northwest continuation of the ECSZ (Figure 11). This deformation may be accommodated by clockwise rotation of the Coast Ranges block (Wells et al., 1998), horizontal contraction of the Klamath Mountains in the form of uplift (Aalto et al., 1991) and westward migration of the coastline (Figure 10). Deformation may be localized within the Klamath Mountains for two basic reasons: they are comprised of weak serpentized ophiolitic rocks in contrast to the stronger "Siletzia" basaltic seamount terrane of the Coast Ranges (Snively and Wells, 1996) immediately to the north; and at the Mendocino Triple Junction to the south, the subduction zone gives way to the transform margin which impedes westward dilation. The absence of prominent faults and seismicity may be because deformation is being distributed aseismically throughout the large serpentized bodies of the ophiolite.

Perhaps the most significant result of this model is the motion of the Coast Range block and its influence on the convergence velocity at the CSZ and location of strain associated with the northern extension of the ECSZ. Simple thoughts about the westward expansion of the Basin and Range and dextral shear associated with the ECSZ would suggest that the Coast Range motion is rapid (clockwise motion about an Euler pole east of the northern end of the block). In addition to the rotation component of motion, a relatively large translation would be required. This rapid motion would also affect the convergence rate at the CSZ. The rapid rotation with the southern end moving west-northwestward would increase the normal component of convergence.

In fact, our preferred model shows that these effects are correct but only to a minor degree. Much of the ECSZ velocity actually escapes through the Klamath Mountain region of northern California (Figure 11) resulting in an Euler pole that is more to the southwest than earlier estimates. As a consequence, the required rapid northward translation of the Coast Range block is diminished.

The model provides a means to estimate convergence velocity along the CSZ. By differencing model nodal velocities on either side of the subduction zone we can calculate convergence velocities. Because we consider the accretionary prism immediately adjacent to the trench to be straining elastically in response to coupling (Hyndman and Wang, 1993; Hyndman and Wang, 1995) we use nodal velocities in the forearc above the coupled zone.

In Figure 15a the resultant vectors for both models are shown along the subduction margin. The plate-rate predicted convergence azimuths remain nearly constant along the length of the subduction zone while the model-derived azimuths diverge. Deformation without the Gorda and Explorer plates is responsible for the large departures in azimuths at

either end of the CSZ. While not well-constrained for the Gorda plate, the Explorer plate deformation described by Kreemer et al. (1998) may be responsible for curiously large margin parallel velocities reported by Dragert and Hyndman (Dragert and Hyndman, 1995) for northern Vancouver Island (Figure 15a).

Because the plate-rate model only considers an Euler pole (to the south) for the JDF plate approaching a stable upper plate, the predicted convergence velocity increases linearly northward along the subduction zone (Figure 15b). The kinematic model suggests that the convergence rate does not increase linearly but instead has a broad zone of nearly consistent velocity (34-37 mm/y) bounded by velocity highs which then decrease rapidly toward the ends of the CSZ. To the south, the velocity increases rapidly across the length of the Gorda plate as a result of internal deformation of the oceanic plate and rapid westward encroachment of the Klamath Mountains and southern Coast Range block. A peak in convergence rate of about 37 mm/y occurs at the southern most JDF plate south of Cape Blanco. The nearly constant convergence rate over much of the length of the JDF plate results from a balance between the clockwise rotation of the oceanic plate about an Euler pole to the south with $\omega = 1.3^\circ/\text{m.y.}$ and the clockwise rotation of the Coast Range block about an Euler pole to the northeast and $\omega = 1.5^\circ/\text{m.y.}$ (Table 1). The convergence velocity increases to the north as the significance of the Coast Range rotation diminishes and the orientation of the CSZ changes.

Differences in the normal and tangential components of the convergence velocities between the two models also exist (Figure 15b). The plate-rate-derived normal velocity increases steadily (at a rate similar to the resultant velocity) toward the north as a result of the position of the Euler pole to the south. The normal velocity actually equals the convergence velocity where the trench bends toward the west between the Olympic Peninsula and Vancouver Island. As the CSZ continues to bend farther toward the west, the normal velocity decreases slightly. Likewise, the kinematic model-derived normal velocity closely resembles the form of the resultant velocity (Figure 15b). It is approximately 7 mm/y greater than the predicted normal velocity near Cape Blanco. The normal velocity remains higher than the predicted velocity up to about latitude 45°N . It equals the resultant velocity at the bend in the CSZ and peaks near the northern end of the JDF plate. It then diminishes rapidly along the Explorer plate.

Except for the ends of the CSZ, the tangential velocities are similar for both models. They both show a significant dextral velocity (up to ~ 15 mm/y) along the southern JDF plate that diminishes toward the bend in the CSZ. Because of the geometry of the bend and plate vector azimuth, margin-parallel sinistral motion of up to ~ 14 mm/y occurs at about latitude 50°N . Dextral motion parallel to the margin once again becomes evident to the north as the Explorer plate accommodates the Pacific plate motion.

In summary, the overall difference between the convergence velocities of the two models is not as large as one might initially guess. There is an increase in the resultant velocity near the southern end of the JDF plate as a result of the escape of the ECSZ through the Klamath Mountains. However, as a result of directing this shear to the south, the Euler vector for the Coast Ranges rotation moves to the west and the northwestward translation of the entire block is less. The opposing rotations of the JDF plate and Coast Ranges result in a convergence rate that is actually lower over most of the subduction zone than predicted by the plate-rate model (Figure 15b).

CONCLUSIONS

The kinematic finite element model provides a method for evaluating deformation across a broad region. It affords insight as to the location, amount and style of deformation in areas where relatively little observational information exists. The model makes use of available information and interpolates between areas of observational constraint in a self-consistent

manner. In areas of poor data coverage, the inclusion of observational constraints will improve model accuracy and certainty.

The accuracy of the model can be verified by comparison of individual block or nodal velocities with observed geodetic and geologic rates.

We have an improved estimate of the convergence velocities across the subduction zone, taking into consideration the deformation of the North American plate in addition to the oceanic plate rate.

The kinematics of western U.S. deformation shows that deformation tends to be directed toward the subduction zone and that the motion of the Coast Ranges, driving over the subduction zone, is accommodating the collapse of the interior.

BIBLIOGRAPHY

- Aalto, K. R., Moley, K., Knudsen, K. L., and Stone, L., 1991, Sediment provenance and Cenozoic tectonic evolution of the central and western Klamath Mountains and northernmost Coast Ranges, California: Geological Society of America, Abstracts with Programs, v. 23, no. 5, p. A137.
- Adams, J., 1990, Paleoseismicity of the Cascadia Subduction Zone: Evidence from turbidites off the Oregon-Washington margin: *Tectonics*, v. 9, p. 569-583.
- Ando, M., and Babazs, E. I., 1979, Geodetic evidence for aseismic subduction of the Juan de Fuca plate: *Journal of Geophysical Research*, v. 84, p. 3123-3028.
- Argus, D. F., and Gordon, R. G., 1991a, Current Sierra Nevada-North America motion from very long baseline interferometry: Implications for the kinematics of the western United States: *Geology*, v. 19, p. 1085-1088.
- Argus, D. F., and Gordon, R. G., 1991b, No-net-rotation model of current plate velocities incorporating plate motion model Nuvel-1: *Geophysical Research Letters*, v. 18, no. 11, p. 2039-2042.
- Argus, D. F., and Gordon, R. G., 1996, Test of the rigid-plate hypothesis and bounds on intraplate deformation using geodetic data from very long baseline interferometry: *Journal of Geophysical Research*, v. 101, no. 6, p. 13,555-13,572.
- Atwater, B. F., 1988, Comment on "Coastline uplift in Oregon and Washington and the nature of Cascadia subduction-zone tectonics: *Geology*, v. 16, no. 10, p. 952.
- Atwater, T., 1970, Implications of plate tectonics for the Cenozoic tectonic evolution of western North America: *Geological Society of America Bulletin*, v. 81, p. 3513-3536.
- Atwater, T., 1989, Plate tectonic history of the northeast Pacific and western North America, in Winterer, E. L., Hussong, D. M., and Decker, R. W., eds., *The Eastern Pacific Ocean and Hawaii*: Boulder, Geological Society of America, p. 21-72.
- Atwater, T., and Stock, J., 1997, Pacific-North America plate tectonics of the Neogene southwestern United States - an update, in *Hall Symposium*.
- Bennett, R. A., Wernicke, B. P., and Davis, J. L., 1998, Continuous GPS measurements of contemporary deformation across the northern Basin and Range province: *Geophysical Research Letters*, v. 25, no. 4, p. 563-566.
- Brandon, M. T., Roden-Tice, M. K., and Garver, J. I., 1998, Late Cenozoic exhumation of the Cascadia accretionary wedge in the Olympic Mountains, northwest Washington State: *Geological Society of America Bulletin*, v. 110, no. 8, p. 985-1009.
- Clague, J. J., and Bobrowsky, P. T., 1994, Evidence for a large earthquake and tsunami 100-400 years ago on western Vancouver Island, British Columbia: *Quaternary Research*, v. 41, p. 176-184.
- Darrienzo, M. E., Peterson, C. D., and Clough, C., 1994, Stratigraphic evidence for great subduction-zone earthquakes at four estuaries in northern Oregon, U.S.A.: *Journal of Coastal Research*, v. 10, no. 4, p. 850-876.
- DeMets, C., Gordon, R. G., Argus, D. F., and Stein, S., 1990, Current plate motions: *Geophysical Journal International*, v. 101, p. 425-478.

- DeMets, C., Gordon, R. G., Argus, D. F., and Stein, S., 1994, Effect of recent revisions to the geomagnetic reversal time scale on estimates of current plate motions: *Geophysical Research Letters*, v. 21, no. 20, p. 2191-2194.
- DeMets, C., Gordon, R. G., Stein, S., and Argus, D. F., 1987, A revised estimate of Pacific-North America motion and implications for western North America plate boundary zone tectonics: *Geophysical Research Letters*, v. 14, p. 911-914.
- Denlinger, R. P., 1992, A model for large-scale plastic yield of the Gorda deformation zone: *Journal of Geophysical Research*, v. 97, no. 11, p. 15,415-15,423.
- Dixon, T. H., Bursik, M., Kornreich Wolf, S., Heflin, M., Webb, F., Farina, F., and Robaudo, S., 1993, Constraints of deformation of the resurgent dome, Long Valley Caldera, California from space geodesy, *in* Smith, D. E., and Turcotte, D. L., eds., *Contributions of Space Geodesy to Geodynamics: Crustal Dynamics*: Washington, D.C., American Geophysical Union, p. 429.
- Dixon, T. H., Robaudo, S., Lee, J., and Reheis, M. C., 1995, Constraints on present day Basin and Range deformation from space geodesy: *Tectonics*, v. 14, no. 4, p. 755-772.
- Dragert, H., and Hyndman, R. D., 1995, Continuous GPS monitoring of elastic strain in the northern Cascadia subduction zone: *Geophysical Research Letters*, v. 22, no. 7, p. 755-758.
- Dumitru, T. A., Gans, P. B., Foster, D. A., and Miller, E. L., 1991, Refrigeration of the western Cordilleran lithosphere during Laramide shallow-angle subduction: *Geology*, v. 19, p. 1145-1148.
- Goldfinger, C., Kulm, L. D., and Yeats, R. S., 1994, An estimate of maximum earthquake magnitude on the Cascadia subduction zone (abstract): *Geological Society of America Abstracts with Programs*, v. 26, no. 7, p. 525.
- Gripp, A. E., and Gordon, R. G., 1990, Current plate velocities relative to the hotspots incorporating the Nuvel-1 global plate motion model: *Geophysical Research Letters*, v. 17, no. 8, p. 1109-1112.
- Hamilton, W. B., 1988, Laramide crustal shortening, *Geological Society of America*, p. 27-39.
- Hearn, E. H., and Humphreys, E. D., 1998, Kinematics of the southern Walker Lane Belt and motion of the Sierra Nevada block, California: *Journal of Geophysical Research*, v. 103, no. B11, p. 27,033-27,049.
- Heaton, T. H., and Hartzell, S. H., 1987, Earthquake hazards on the Cascadia subduction zone: *Science*, v. 236, p. 162-236.
- Hemphill-Haley, M. A., Page, W. D., Carver, G. A., and Burke, R. M., 1998a, Paleoseismicity of the Alvord Fault, Steens Mountain, southeastern Oregon, *in* Sowers, J. M., Noller, J. S., and Lettis, W. R., eds., *Dating and Earthquakes: Review of Quaternary Geochronology and its Application to Paleoseismology*, U.S. Nuclear Regulatory Commission, p. 3.89-3.95.
- Hemphill-Haley, M. A., Sawyer, T. L., Knuepfer, P. L. K., Forman, S. L., and Wong, I. G., 1998b, Timing of faulting events from thermoluminescence dating of scarp-related deposits, Lemhi fault, southeastern Idaho, *in* Sowers, J. M., Noller, J. S., and Lettis, W. R., eds., *Dating and Earthquakes: Review of Quaternary Geochronology and its Application to Paleoseismology*, U.S. Nuclear Regulatory Commission, p. 3.97-3.105.
- Hemphill-Haley, M. A., Weldon, R. J., II, Langridge, R. L., and Stimac, J. P., 1996, Late Pleistocene and Holocene faulting and volcanism along the back- and intra-arc regions of the Cascadia Subduction Zone, Oregon: *Geological Society of America, Abstracts with Programs*, v. 28, no. 5, p. 74.
- Hooper, P. R., and Conrey, R. M., 1989, The Olympic-Wallowa-lineament (OWL) as a Basin and Range-related megashear, and its control of magmatism during the eruption of the Columbia River basalts: *Geological Society of America, Abstracts with Programs*, v. 21, no. 5, p. 94.

- Humphreys, E. D., 1995, Post-Laramide removal of the Farallon slab, western United States: *Geology*, v. 23, no. 11, p. 987-990.
- Humphreys, E. D., and Weldon, R. J., II, 1994, Deformation across the western United States: A local estimate of Pacific-North America transform deformation: *Journal of Geophysical Research*, v. 99, no. B10, p. 19,975-20,010.
- Hyndman, R. D., and Wang, K., 1993, Thermal constraints on the zone of major thrust earthquake failure: the Cascadia Subduction Zone: *Journal of Geophysical Research*, v. 98, no. B2, p. 2039-2060.
- Hyndman, R. D., and Wang, K., 1995, The rupture zone of Cascadia great earthquakes from current deformation and the thermal regime: *Journal of Geophysical Research*, v. 100, p. 22,133-22,154.
- Jones, C., Unruh, J. R., and Sonder, L. J., 1996, The role of gravitational potential energy in active deformation in the southwestern United States: *Nature*, v. 381, p. 37-41.
- Kelsey, H. M., 1990, Late Quaternary deformation of marine terraces on the Cascadia subduction zone near Cape Blanco, Oregon: *Tectonics*, v. 9, no. 5, p. 983-1014.
- Kelsey, H. M., Witter, R. C., Nelson, A. R., and Hemphill-Haley, E., 1994, Repeated abrupt late Holocene environmental change in south coastal Oregon: Stratigraphic evidence at Sixes River marsh and Bradley Lake (abstract): *Geological Society of America Abstracts with Programs*, v. 26, no. 7, p. 524.
- Kreemer, C., Govers, R., Furlong, K. P., and Holt, W. E., 1998, Plate boundary deformation between the Pacific and North America in the Explorer region: *Tectonophysics*, v. 293, p. 225-238.
- Lisowski, M., Savage, J. C., and Prescott, W. H., 1987, Strain accumulation along the Cascadia subduction zone in western Washington: *Eos, Transactions of the American Geophysical Union*, v. 68, p. 1240.
- Livaccari, R. F., 1991, Role of crustal thickening and extensional collapse in the tectonic evolution of the Sevier-Laramide orogeny, western United States: *Geology*, v. 19, p. 1104-1107.
- Madin, I. P., Hemphill-Haley, M. A., and Roberts, T., 1994, Late Quaternary faulting in the South Slough area, Coos County Oregon: .
- Magill, J. R., Wells, R. E., Simpson, R. W., and Cox, A. V., 1982, Post 12 m.y. rotation of southwest Washington: *Journal of Geophysical Research*, v. 87, p. 3761-3776.
- Mann, G. M., 1991, Structure and correlations to seismicity along the Olympic-Wallowa Lineament: *EOS Transactions, American Geophysical Union*, v. 72, no. 44, p. 315.
- Martinez, L. J., Meertens, C. M., and Smith, R. B., 1998, Rapid deformation rates along the Wasatch fault zone, Utah, from first GPS measurements with implications for earthquake hazard: *Geophysical Research Letters*, v. 25, no. 4, p. 567-570.
- McCaffrey, R., and Goldfinger, C., 1995, Forearc deformation and great subduction earthquakes: Implications for Cascadia offshore earthquake potential: *Science*, v. 267, p. 856-859.
- McCrory, P. A., 1996, Tectonic model explaining divergent contraction directions along the Cascadia subduction margin, Washington: *Geology*, v. 24, no. 10, p. 929-932.
- Minster, J. B., and Jordan, T. H., 1987, Vector constraints on the western U.S. deformation from space based geodesy, neotectonics, and plate motions: *Journal of Geophysical Research*, v. 92, p. 4798-4808.
- Mitchell, C., Vincent, P., Weldon, R. J., II, and Richards, M. A., 1994, Present-day vertical deformation of the Cascadia margin, Pacific Northwest, United States: *Journal of Geophysical Research*, v. 99, no. B6, p. 12,257-12,277.
- Nelson, A. R., and Personius, S. F., 1991, Great earthquake potential in Oregon and Washington -- An overview of recent coastal geologic studies and their bearing on segmentation of Holocene ruptures in the central Cascadia subduction zone, *in* Rogers, A. M., Kockelman, W. J., Priest, G., and Walsh, T. J., eds., *Assessing and Reducing Earthquake Hazards in the Pacific Northwest, U.S. Geological Survey Open-File Report 91-441A*, p. 1-29.

- Pezzopane, S. K., 1993, Active Faults and Earthquake Ground Motions in Oregon [Ph.D. thesis]: University of Oregon, 208 p.
- Pezzopane, S. K., and Weldon, R. J., II, 1993, Tectonic role of active faulting in central Oregon: *Tectonics*, v. 12, no. 5, p. 1140-1169.
- Reilinger, R. E., and Adams, J., 1992, Geodetic evidence for active landward tilting of the Oregon and Washington coastal ranges: *Geophysical Research Letters*, v. 9, p. 401-403.
- Riddihough, R., 1984, Recent movements of the Juan de Fuca plate system: *Journal of Geophysical Research*, v. 89, p. 6980-6994.
- Rogers, G. C., 1987, Vertical motions in the Vancouver Island region: Possible evidence for a megathrust earthquake environment (abs.): *Eos, Transactions of the American Geophysical Union*, v. 68, no. 44, p. 1468.
- Rogers, G. C., 1988, An assessment of the megathrust earthquake potential of the Cascadia subduction zone: *Canadian Journal of Earth Sciences*, v. 25, p. 844-852.
- Saucier, F., and Humphreys, E., 1993, Horizontal crustal deformation in southern California from joint models of geologic and very long baseline interferometry measurements, *in* Smith, D. E., and Turcotte, D. L., eds., *Contributions of Space Geodesy to Geodynamics: Crustal Dynamics*: Washington, D.C., American Geophysical Union, p. 429.
- Savage, J. C., 1983, Strain accumulation in the western United States: *Annual Review of Earth and Planetary Science Letters*, v. 11, p. 11-43.
- Savage, J. C., and Burford, R. O., 1970, Accumulation of tectonic strain in California: *Bulletin of the Seismological Society of America*, v. 60, no. 6, p. 1877-1896.
- Savage, J. C., and Lisowski, M., 1991, Strain measurements and the potential for a great subduction earthquake off the coast of Washington: *Science*, v. 252, p. 101-103.
- Savage, J. C., Lisowski, M., and Prescott, W. H., 1983, Geodetic strain measurements in Washington: *Journal of Geophysical Research*, v. 88, p. 4984-4996.
- Savage, J. C., Lisowski, M., and Prescott, W. H., 1991, Strain accumulation in western Washington: *Journal of Geophysical Research*, v. 96, p. 14,493-14,507.
- Savage, J. C., Lisowski, M., Svarc, J. L., and Gross, K. K., 1995, Strain accumulation across the central Nevada seismic zone: *Journal of Geophysical Research*, v. 100, p. 20,257-20,269.
- Savage, J. C., and Plafker, G., 1991, Tide gage measurements of uplift along the south coast of Alaska: *Journal of Geophysical Research*, v. 96, no. B3, p. 4325-4335.
- Severinghaus, J., and Atwater, T., 1990, Cenozoic geometry and thermal state of the subducting slabs beneath western North America, *in* Wernicke, B. P., ed., *Basin and Range Extensional Tectonics Near the Latitude of Las Vegas, Nevada*: Boulder, Colorado, p. 1-22.
- Shen-Tu, B., Holt, W. E., and Haines, A. J., 1998, Contemporary kinematics of the western United States determined from earthquake moment tensors, very long baseline interferometry, and GPS observations: *Journal of Geophysical Research*, v. 103, no. B8, p. 18,087-18,117.
- Simpson, G. D., Hemphill-Haley, M. A., Wong, I. G., Bott, J. D., Silva, W. J., and Lettis, W. R., 1993, Seismotectonic Evaluation, Burnt River Project-Unity Dam and Baker Project-Thief Valley Dam, Northwestern Oregon: William Lettis & Associates and Woodward-Clyde Federal Services.
- Smith, R. B., and Braile, L. W., 1993, Topographic signature, space-time evolution, and physical properties of the Yellowstone-Snake River Plain volcanic system: the Yellowstone hotspot, *in* Snoke, A. W., Steidtmann, J. R., and Roberts, S. M., eds., *Geology of Wyoming*, Geological Survey of Wyoming, p. 694-754.
- Snively, P. D., Jr., and Wells, R. E., 1996, Cenozoic evolution of the continental margin of Oregon and Washington, *in* Rogers, A. M., Walsh, T. J., Kockelman, W. J., and Priest, G. R., eds., *Assessing Earthquake Hazards and Reducing Risk in the Pacific Northwest*, U.S. Geological Survey, p. 161-182.

- Stoddard, P. R., 1987, A kinematic model for the evolution of the Gorda Plate: *Journal of Geophysical Research*, v. 92, p. 11,524-11,532.
- Stoddard, P. R., 1991, A comparison of brittle deformation models for the Gorda Plate: *Tectonophysics*, v. 187, no. 1-3, p. 205-214.
- Unruh, J. R., and Lettis, W. R., 1998, Kinematics of transpressional deformation in the eastern San Francisco Bay region, California: *Geology*, v. 26, no. 1, p. 19-22.
- Unruh, J. R., Wong, I. G., Bott, J. D. J., Silva, W. J., and Lettis, W. R., 1994, Seismotectonic Evaluation: Scoggins Dam, Tualatin Project, Northwestern Oregon: William Lettis & Associates and Woodward-Clyde Federal Services.
- van der Lee, S., and Nolet, G., 1997, Upper mantle S velocity structure of North America: *Journal of Geophysical Research*, v. 102, no. B-10, p. 22,815-22,838.
- Verdonck, D., 1995, Three-dimensional model of vertical deformation at the southern Cascadia subduction zone, western United States: *Geology*.
- Wang, K., 1996, Simplified analysis of horizontal stresses in a buttressed forearc sliver at an oblique subduction zone: *Geophysical Research Letters*, v. 23, no. 16, p. 2021-2024.
- Wang, K., Mulder, T., Rogers, G. C., and Hyndman, R. D., 1995, Case for very low coupling stress on the Cascadia subduction fault: *Journal of Geophysical Research*, v. 100, p. 12,907-12,918.
- Weldon, R. J., II, 1991, Active tectonic studies in the United States, 1987-1990: *Reviews of Geophysics*, Supplement, p. 890-906.
- Wells, R. E., Weaver, C. S., and Blakely, R. J., 1998, Fore-arc migration in Cascadia and its neotectonic significance: *Geology*, v. 26, no. 8, p. 759-762.
- West, D. O., and McCrumb, D. R., 1988, Coastline uplift in Oregon and Washington and the nature of Cascadia subduction-zone tectonics: *Geology*, v. 16, p. 169-172.
- West, M. W., Ashland, F. X., Busacca, A. J., Berger, G. W., and Shaffer, M. E., 1996, Late Quaternary deformation, Saddle Mountains anticline, south-central Washington: *Geology*, v. 24, no. 12, p. 1123-1126.
- Wilson, D. S., 1989, Deformation of the so-called Gorda Plate: *Journal of Geophysical Research*, v. 94, no. 3, p. 3065-3075.
- Yelin, T. S., and Patton, H. J., 1991, Seismotectonics of the Portland, Oregon, region: *Bulletin of the Seismological Society of America*, v. 81, p. 109-130.

Table 1 - Displacements applied as boundary constraints to the preferred model.

Station Name	Number in Figure 7	Azimuth (°)	Velocity (mm/y)	Station Name	Number in Figure 7	Azimuth (°)	Velocity (mm/y)	ω (°/ma)
Pacific Plate (north)	1	323.5	49.9	Pacific Plate (south)	2	312.9	53.8	0.75
Explorer Plate (north)	3	10	20.0	Explorer Plate (south)	4	20.0	24.2	5.75
Juan de Fuca Plate (north)	5	61.6	42.3	Juan de Fuca Plate (south)	6	57.2	37.1	1.3
Sierra Nevada (Quincy)	7	306.7	12.2	Sierra Nevada (~OVRO)	8	309.9	11.9	0.16
PNW-Coast Range (north)	9	340.0	3.0	PNW-Coast Range (south)	10	295.0	7.0	1.5
John Day Region	11	310.0	3.5	John Day Region (south)	12	320.0	3.7	0.4
Eastern Snake River Plain (east)	13	230.0	3.0	Eastern Snake River Plain (west)	14	235.0	3.0	0.44
Panga-Pentictin	15	350.0	1.0	Panga	16	345.0	0.5	0.02
Colorado Plateau-Pietown	17	290.0	1.0	Colorado Plateau-Flagstaff	18	310.0	1.1	0.09
Idaho Batholith (north)	19	300.0	1.0	Idaho Batholith (south)	20	285.0	1.5	0.2

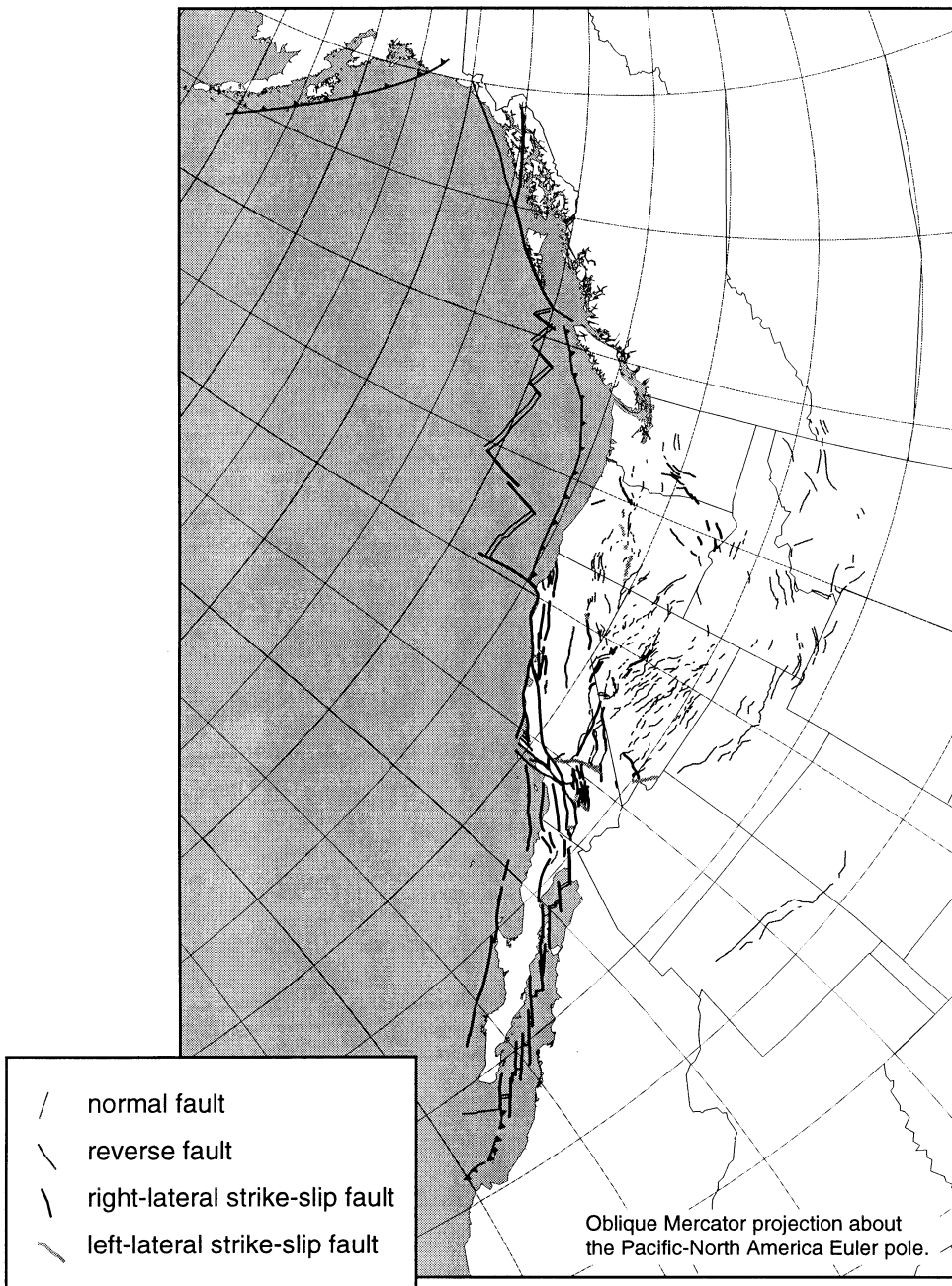


Figure 1 - Late Cenozoic faults within the western United States and adjacent oceanic plates.

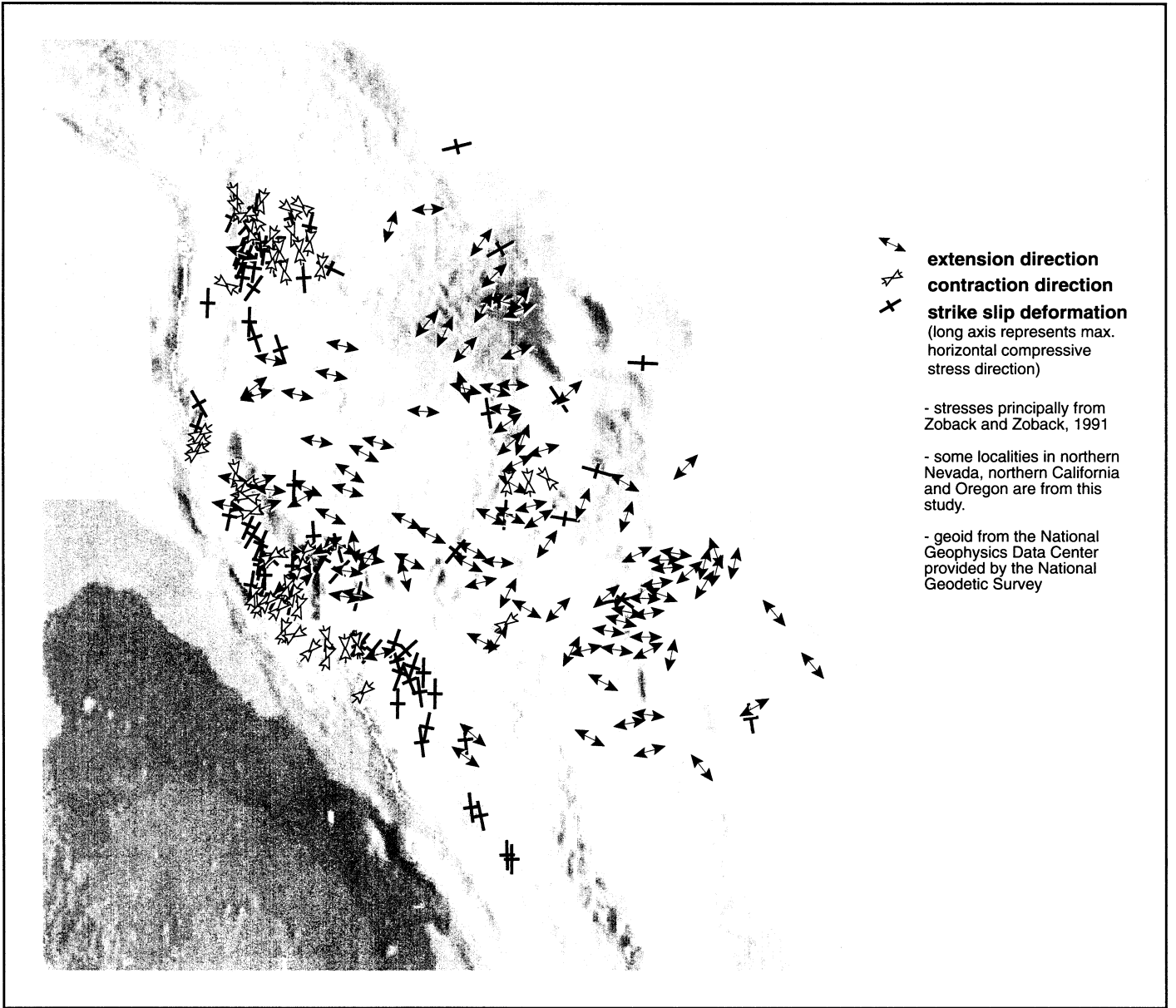


Figure 2 - Late Cenozoic strain superimposed on the geoid for a portion of western North America. The geoid is being used as a proxy for potential energy. Notice that extension diverges from potential energy highs and contraction covers toward potential energy lows. Also, the transform margin accommodates shear while buttressing Basin and Range expansion.

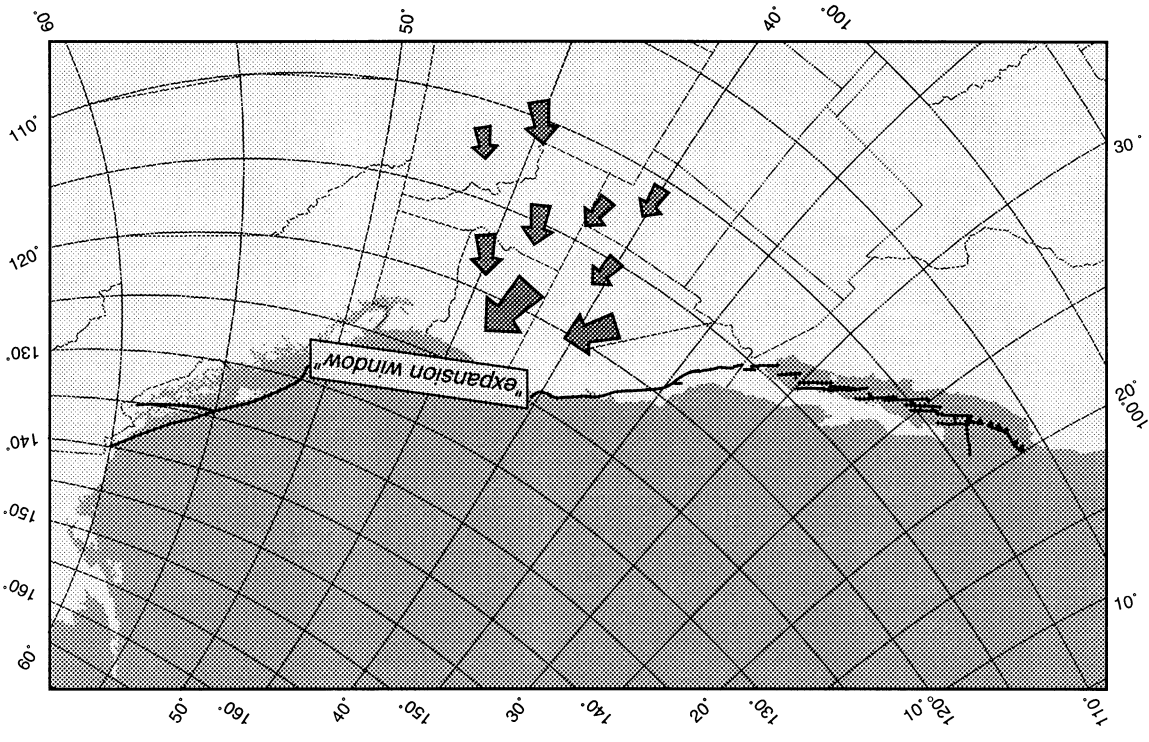
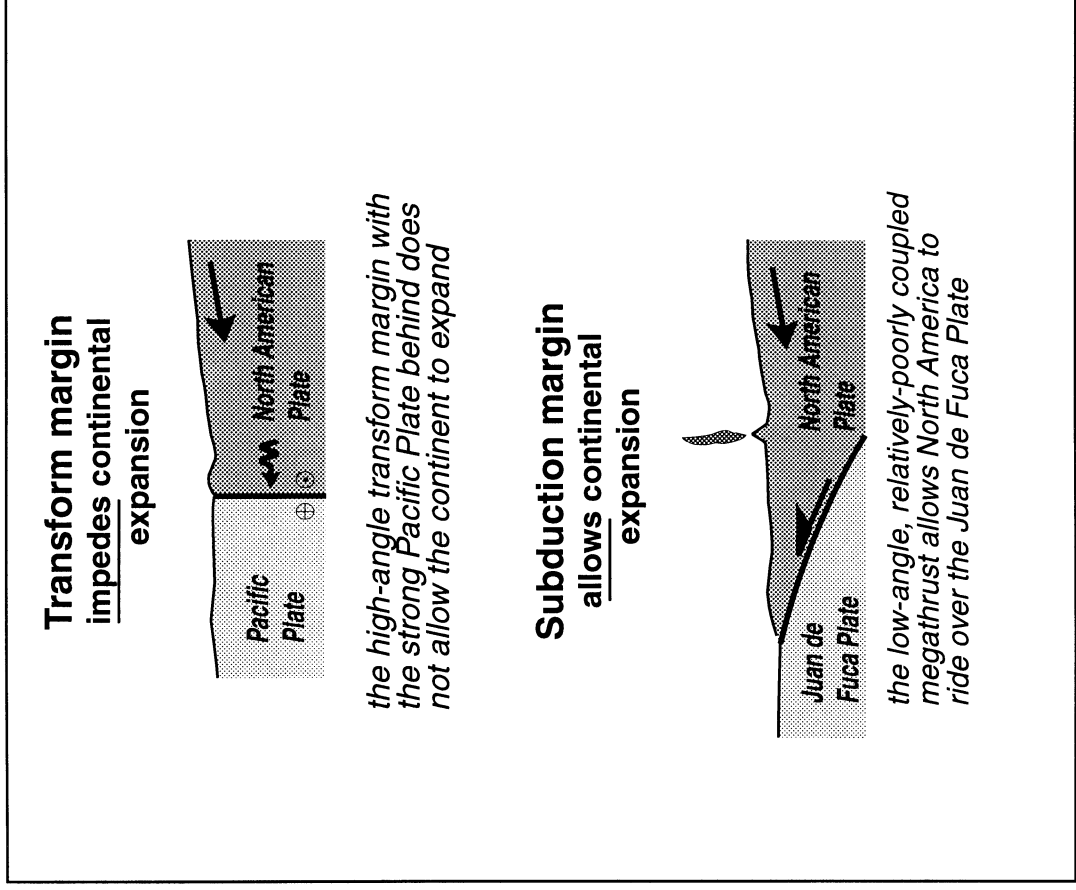


Figure 3 - Diagram showing the reason the expanding interior of the Western U.S. escapes through the Cascadia Subduction Zone. A) Schematic cross-section of the margin of western North America with a transform margin (top) and subduction margin (bottom). The high-angle transform margin backed by the strong Pacific Plate does not allow the continent to expand and locally induces contraction. The low-angle, relatively-poorly coupled megathrust allows North America to "ride" over the oceanic plates. B) The location of the subduction zone "expansion window" relative to approximate extension directions within the continental interior. The implication for this configuration is that the flow of expanding lithosphere is toward the subduction zone and not toward the transform margin .

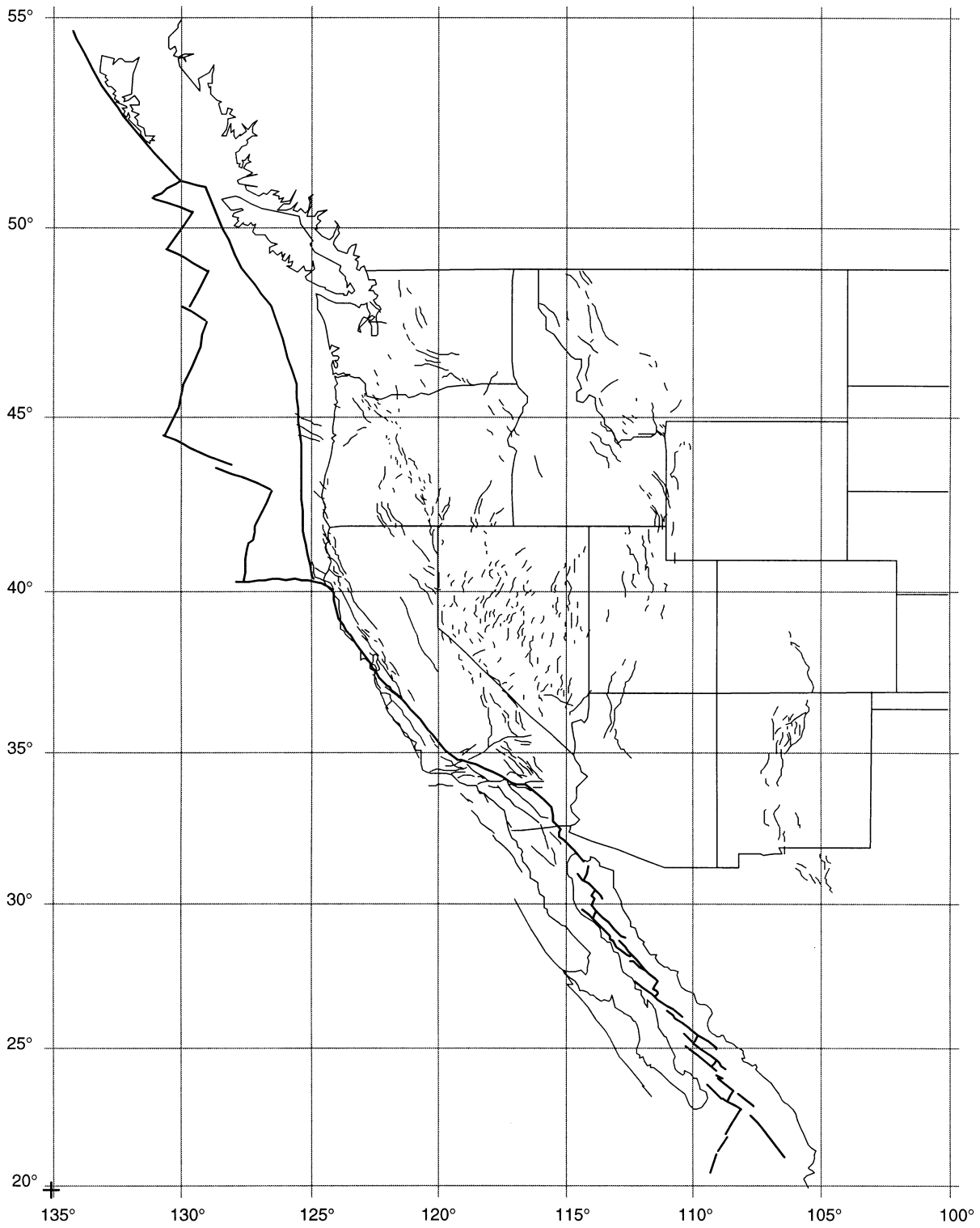


Figure 4 - Framework of the finite element model.

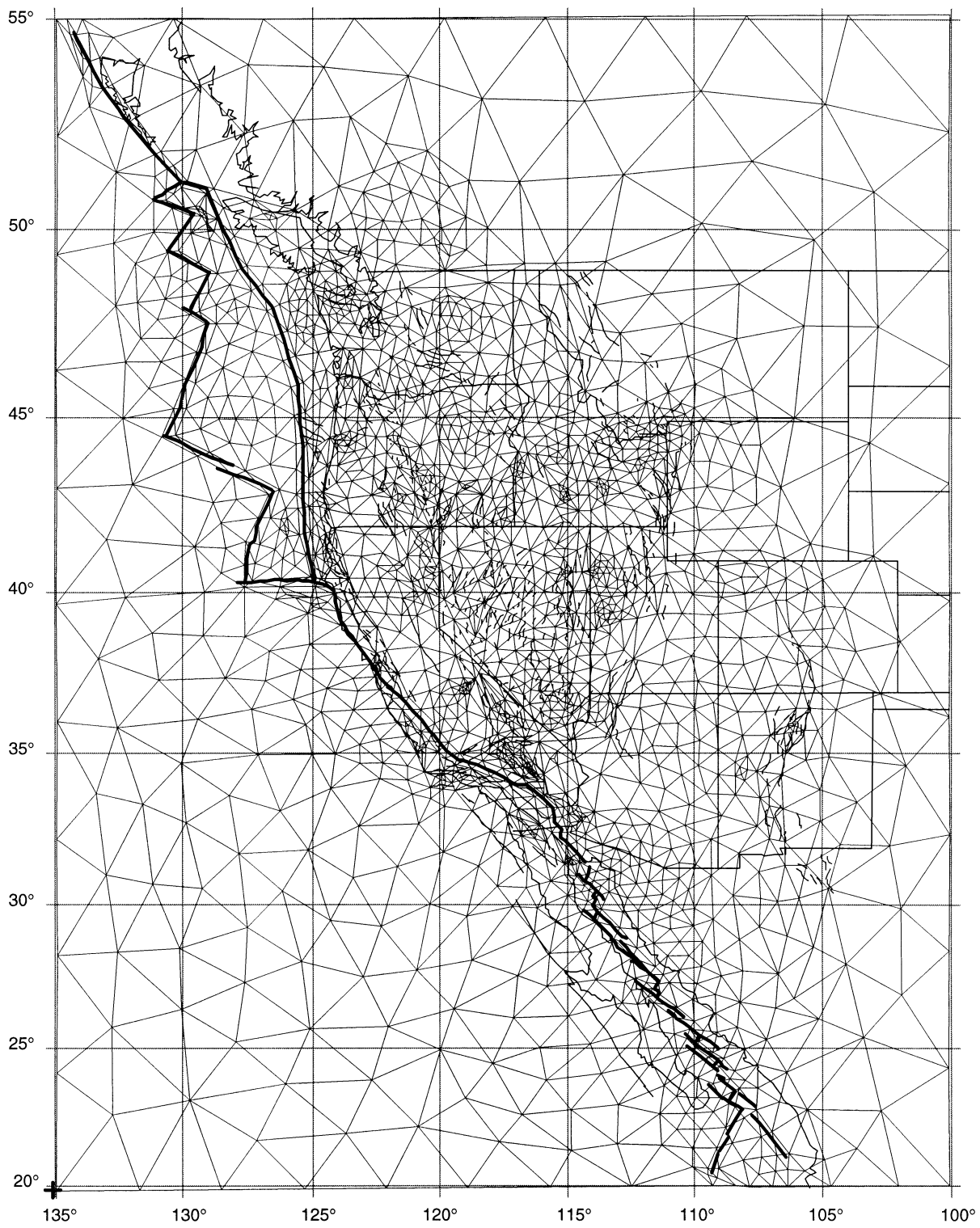


Figure 5 - Finite element grid constructed over model framework.

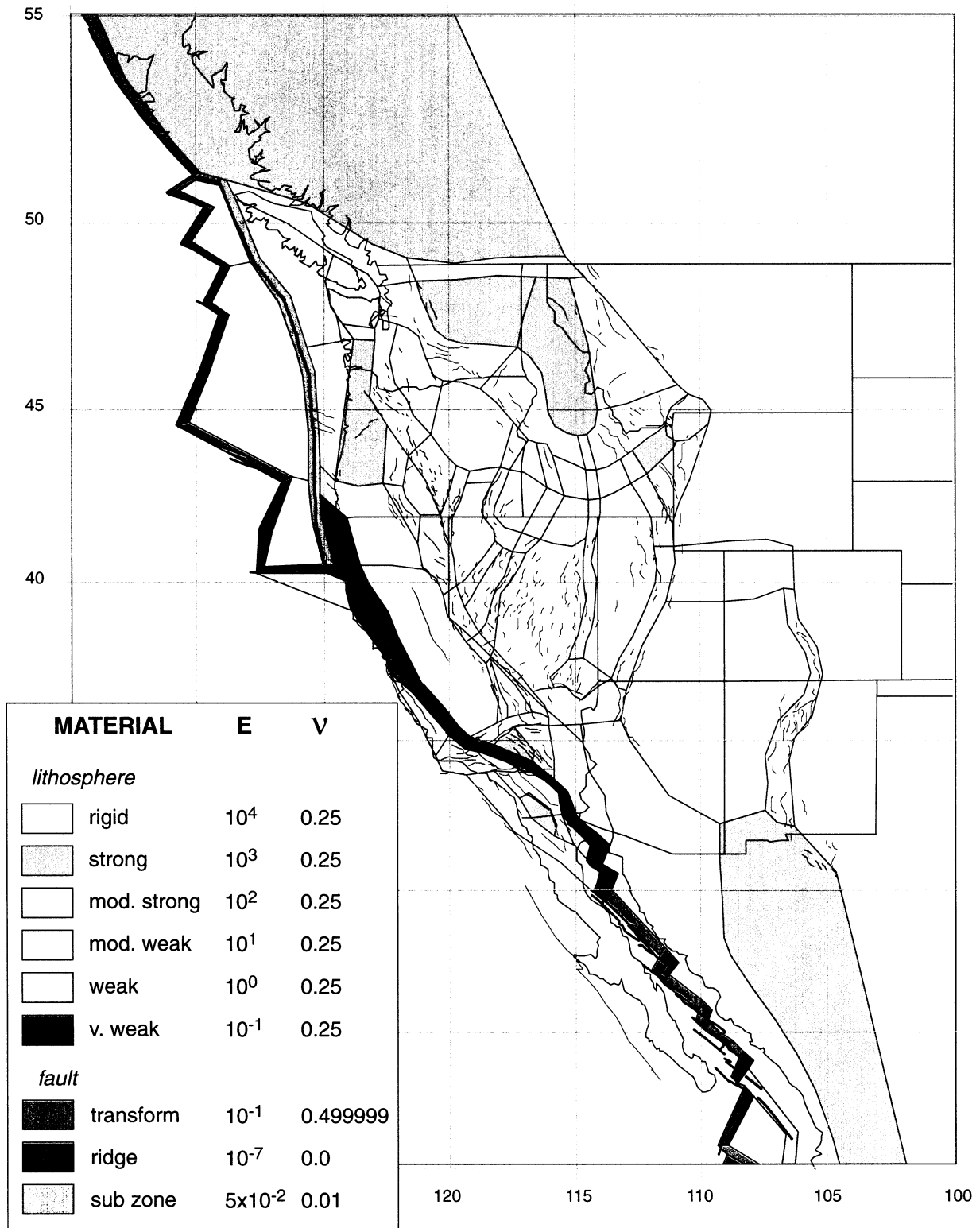


Figure 6- Map showing material property assignments for model components. Material properties based on Young's Modulus (E) and Poisson's Ratio (v).

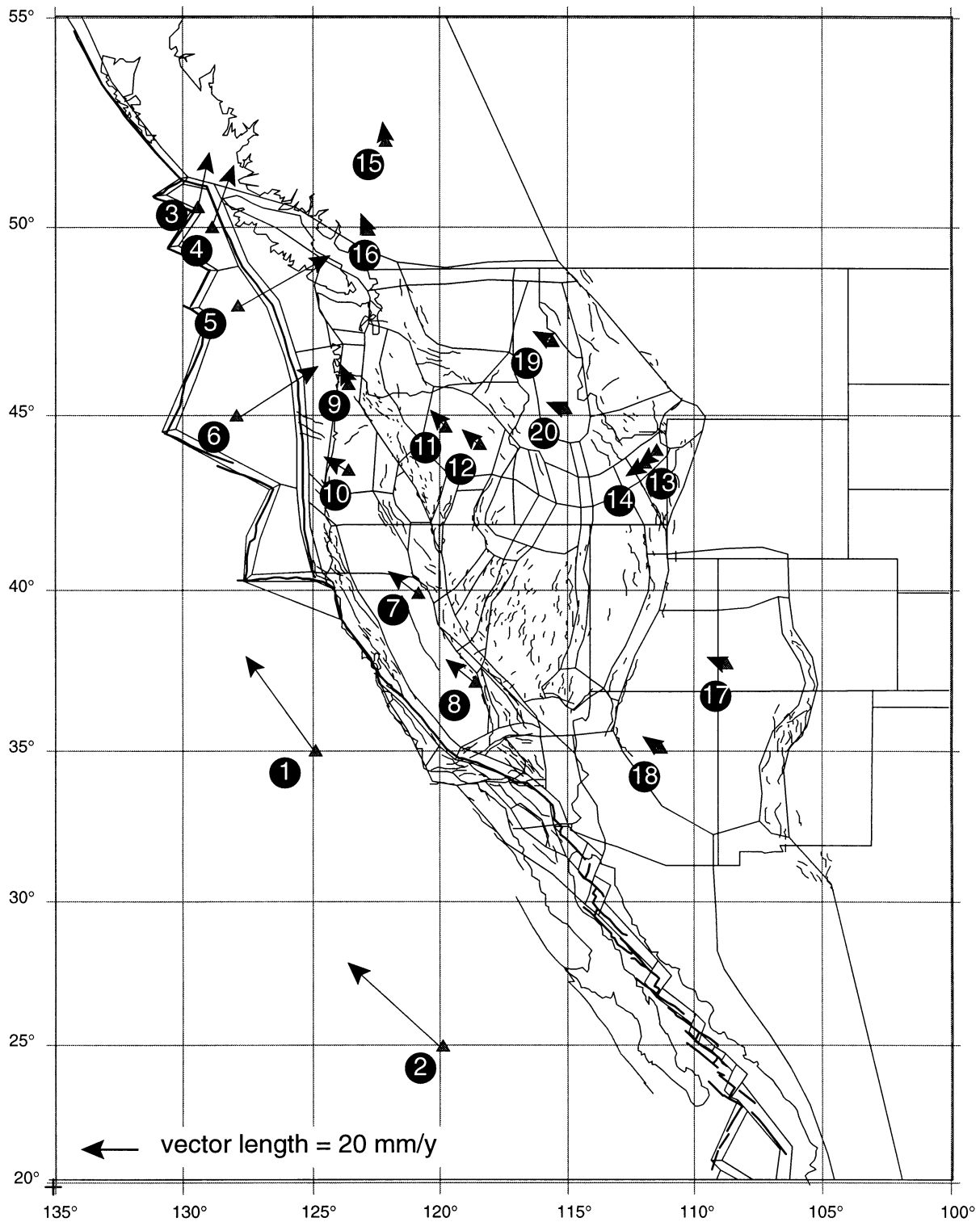


Figure 7 - Velocities applied to the finite element model. Circled numbers adjacent to arrows correspond to velocities reported in Table 1. Triangles show the locations of velocity application points.

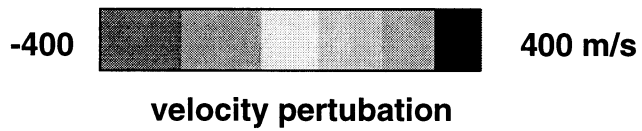


Figure 8 - Mantle velocity at 120 km depth. Higher velocities (cooler colors) correspond to greater strength while lower velocities (warmer colors) are generally associated with weaker mantle. Modified from van der Lee and Nolet, 1997.

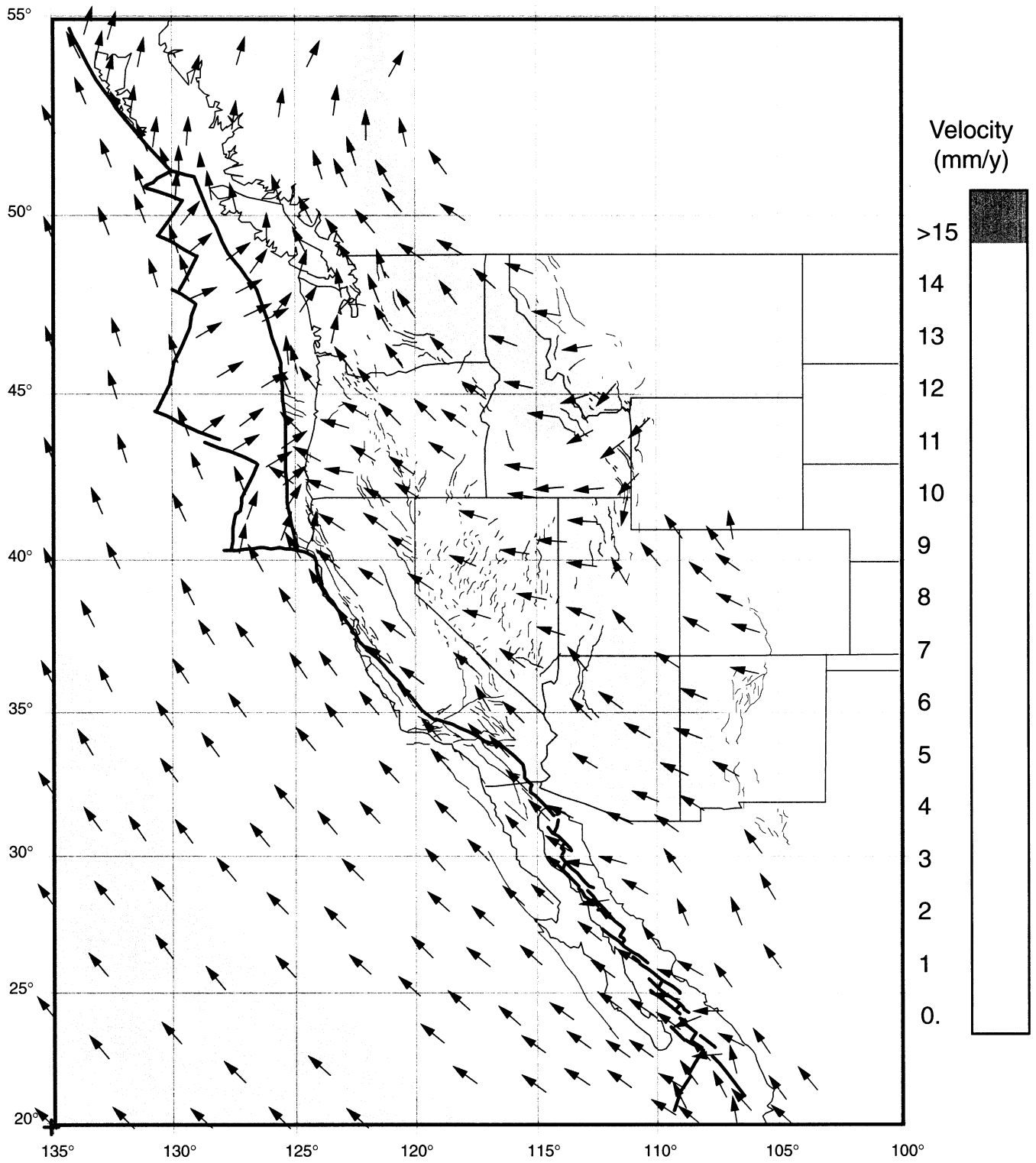


Figure 9 - Velocity map associated with our preferred model. Velocity is contoured by color.

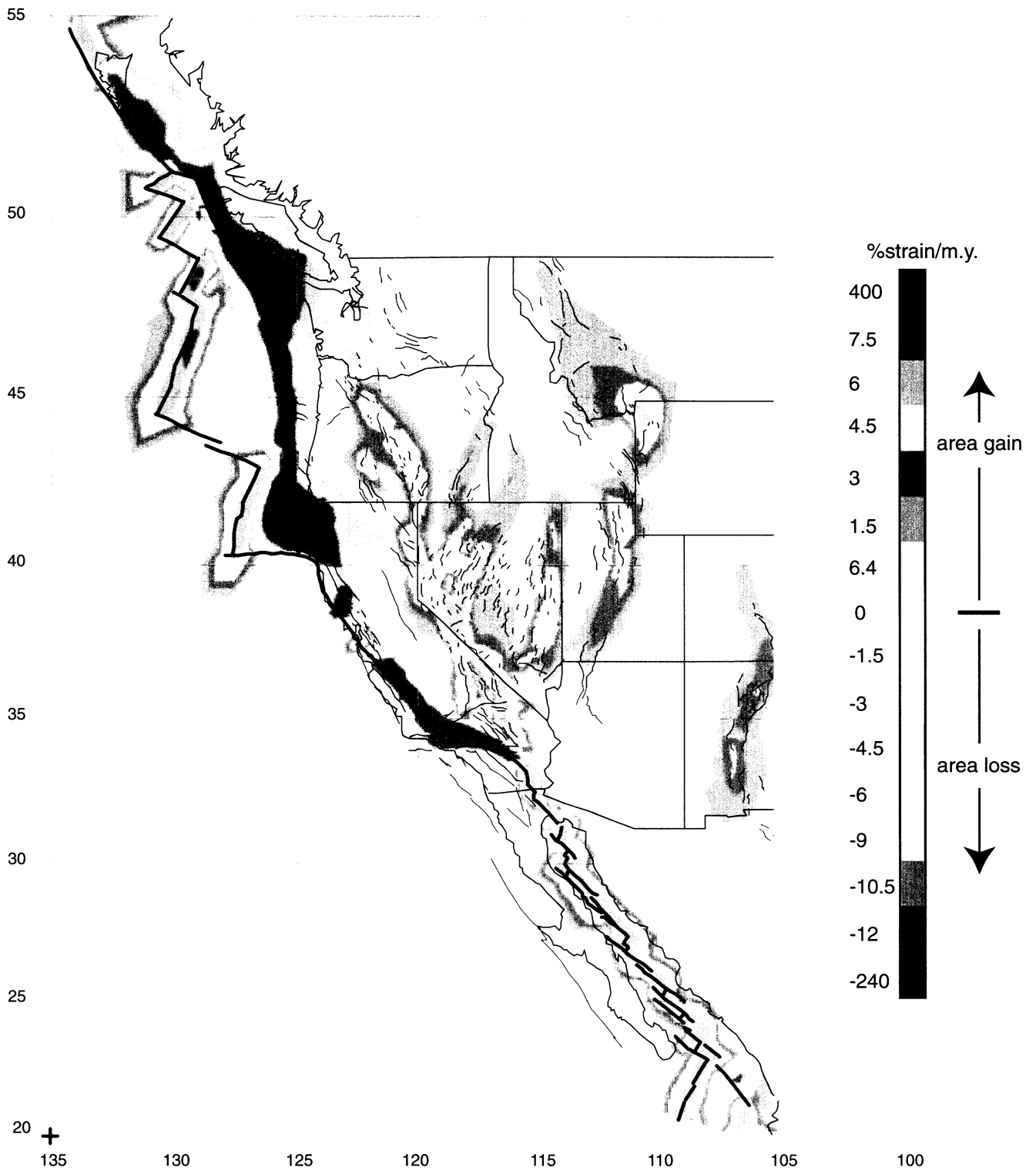


Figure 10 - Map of isotropic strain as a result of the preferred model.

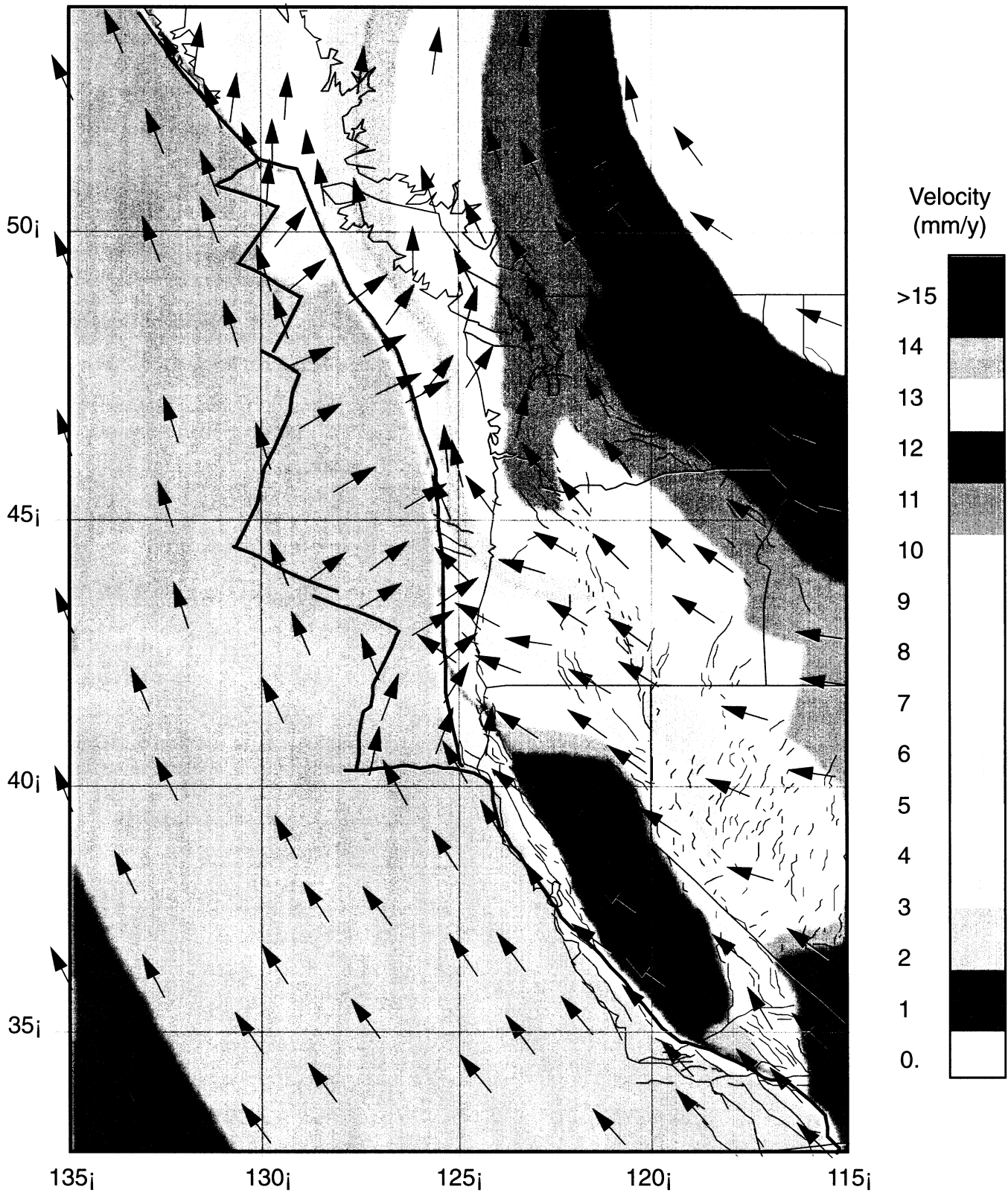


Figure 11 - Enlarged velocity map associated with our preferred model. Velocity is contoured by color.

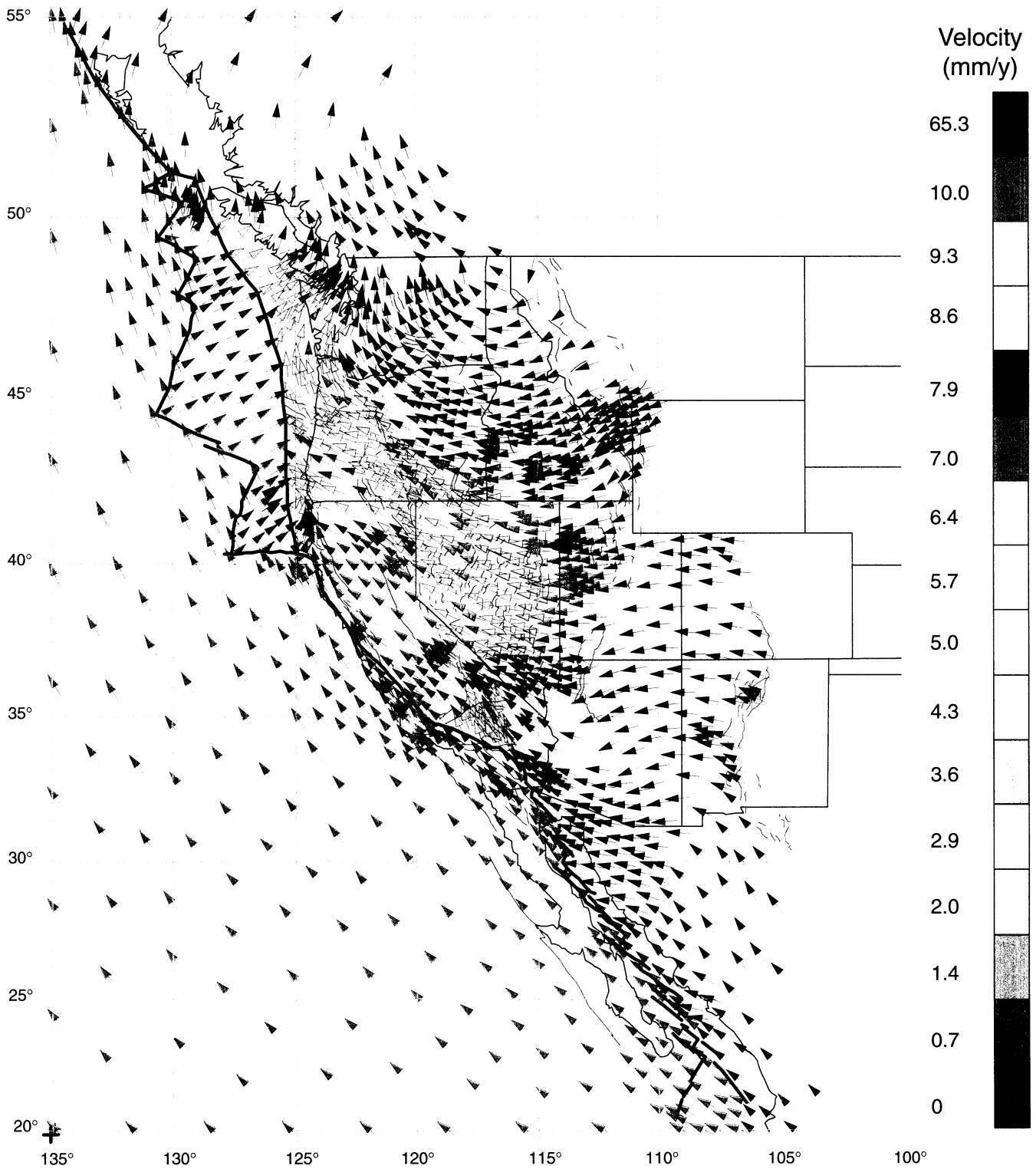


Figure 12 - Velocity field produced when initial conditions do not include velocities related to gravitational collapse of the interior.

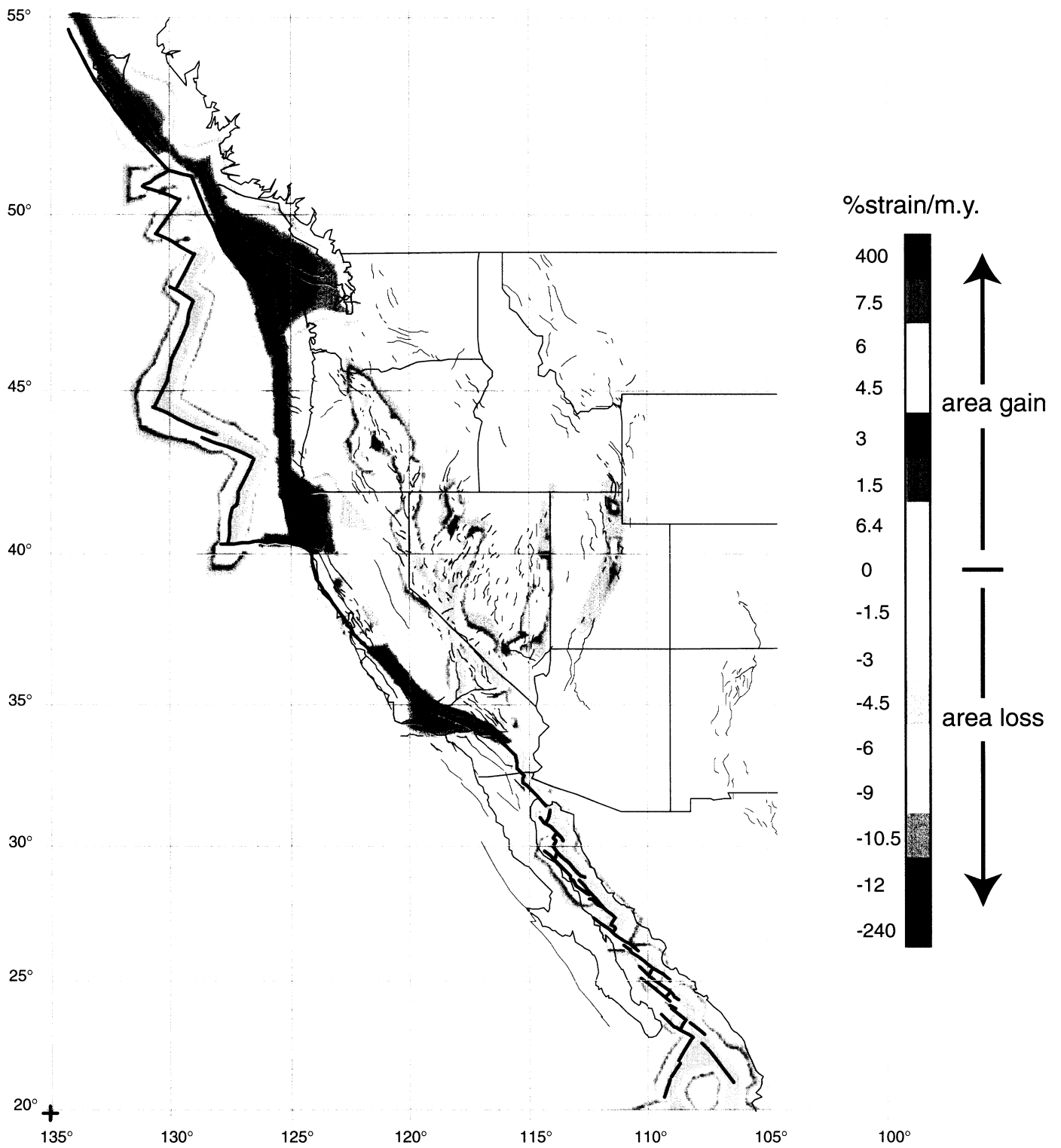


Figure 13 - Isotropic strain map. Velocities associated with gravitational collapse have not been imposed.

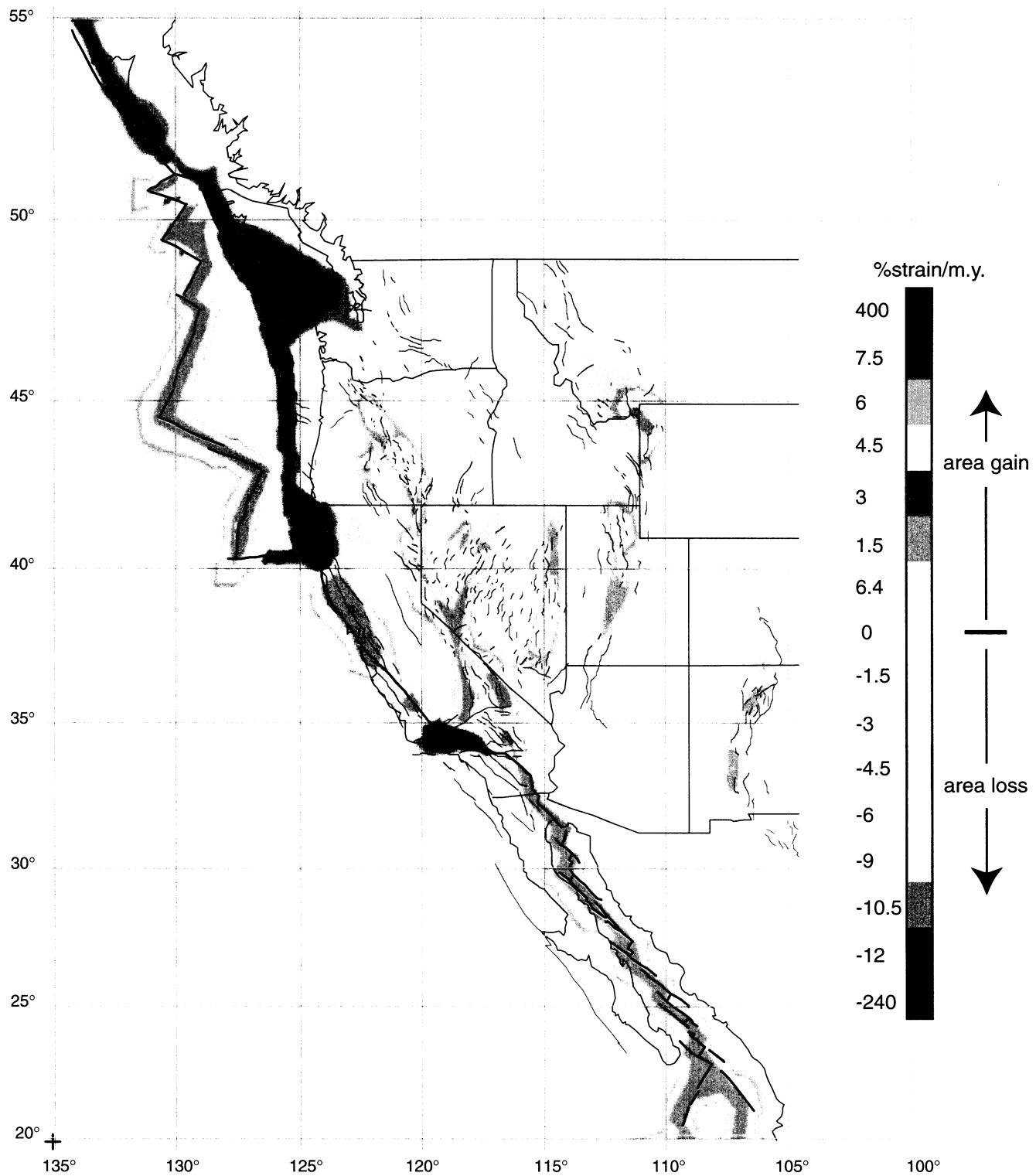
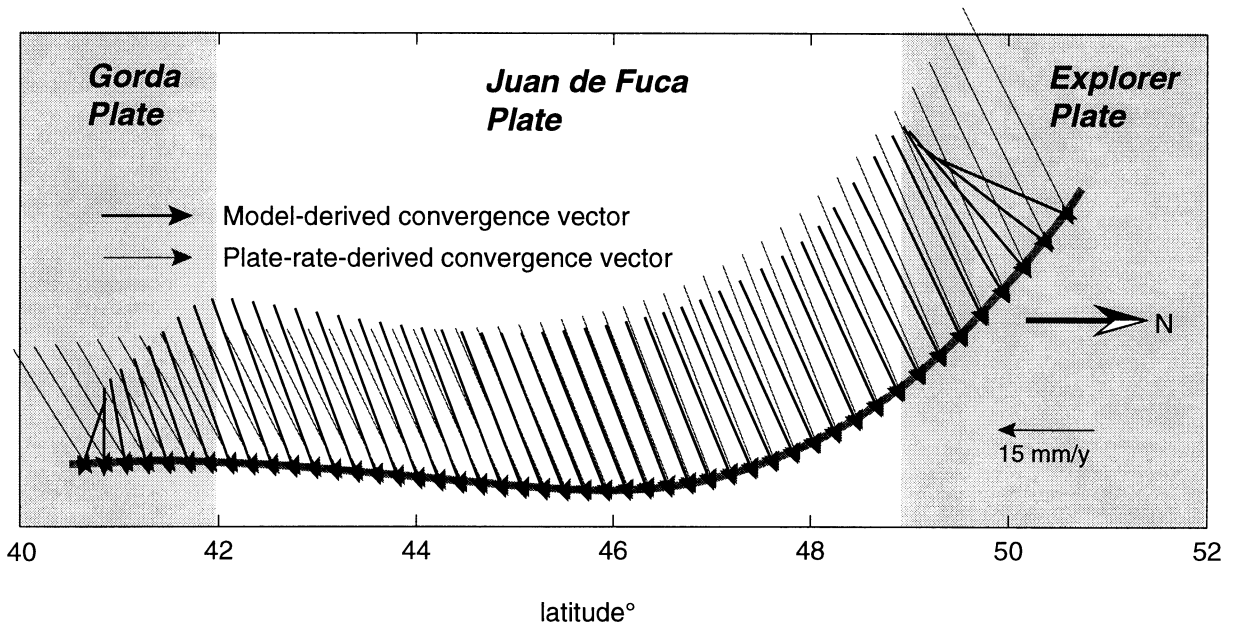
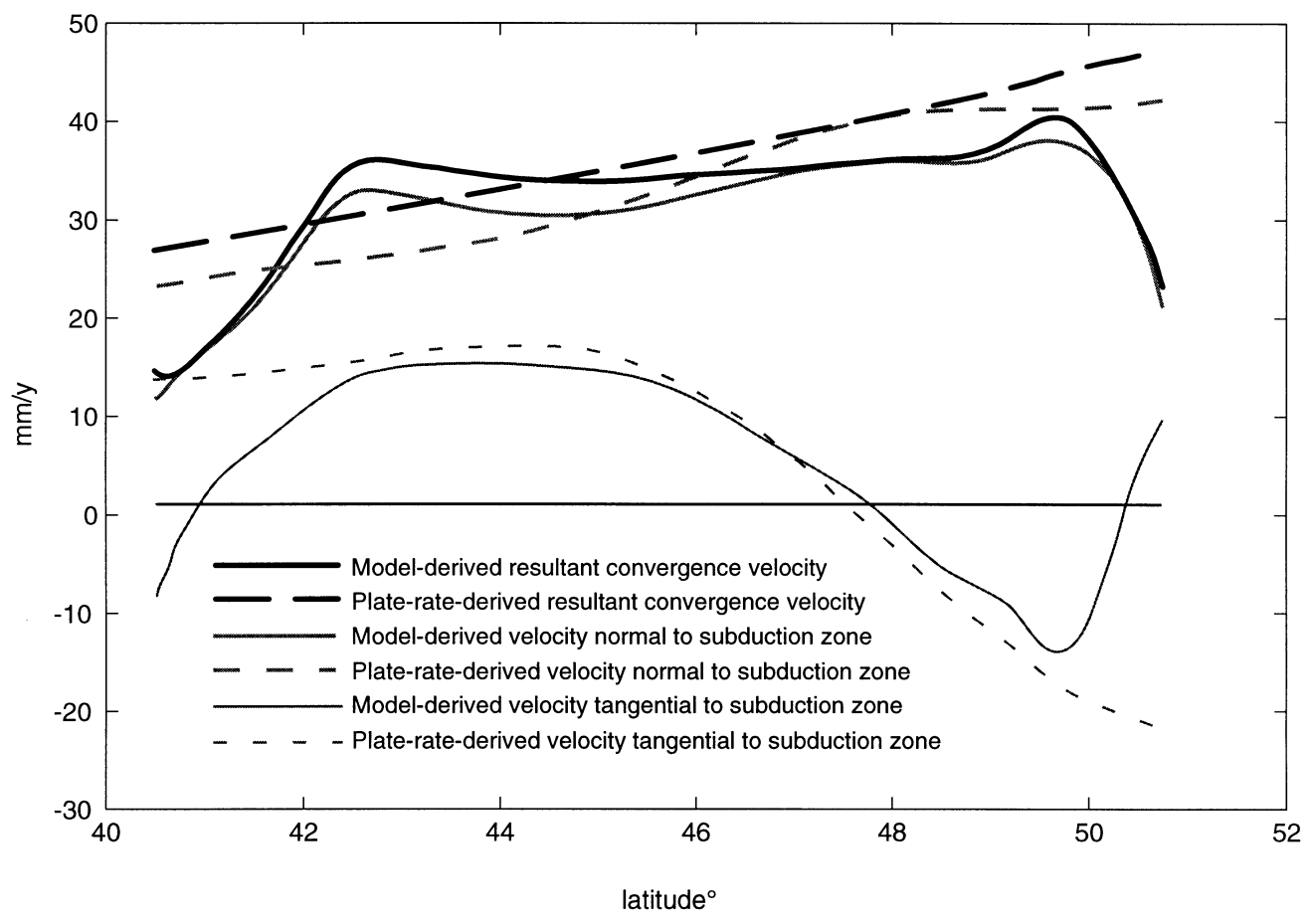


Figure 14 - Map of isotropic strain based on Pacific Plate motion defined by Humphreys and Weldon (1994).



a)



b)

Figure 15 - Convergence velocities between the Juan de Fuca and North America plates along the Cascadia Subduction Zone. a) Resultant velocity azimuths for plate-rate and model-derived rates. b) Velocity components for plate-rate and model-derived rates.